

Utah State University

DigitalCommons@USU

All Graduate Theses and Dissertations


Graduate Studies

8-2011

Studies of the Distinguishing Features of NADPH:2-Ketopropyl-Coenzyme M Oxidoreductase/Carboxylase, an Atypical Member of the Disulfide/ Oxidoreductase Family of Enzymes

Melissa A. Beighley-Kofoed
Utah State University

Follow this and additional works at: <https://digitalcommons.usu.edu/etd>

 Part of the [Biochemistry, Biophysics, and Structural Biology Commons](#)

Recommended Citation

Beighley-Kofoed, Melissa A., "Studies of the Distinguishing Features of NADPH:2-Ketopropyl-Coenzyme M Oxidoreductase/Carboxylase, an Atypical Member of the Disulfide/ Oxidoreductase Family of Enzymes" (2011). *All Graduate Theses and Dissertations*. 1012.

<https://digitalcommons.usu.edu/etd/1012>

This Dissertation is brought to you for free and open access by the Graduate Studies at DigitalCommons@USU. It has been accepted for inclusion in All Graduate Theses and Dissertations by an authorized administrator of DigitalCommons@USU. For more information, please contact digitalcommons@usu.edu.



STUDIES OF THE DISTINGUISHING FEATURES OF NADPH:2-KETOPROPYL-
COENZYME M OXIDOREDUCTASE/CARBOXYLASE, AN ATYPICAL MEMBER
OF THE DISULFIDE OXIDOREDUCTASE FAMILY OF ENZYMES

by

Melissa Kofoed

A dissertation submitted in partial fulfillment
of the requirements for the degree of

DOCTOR OF PHILOSOPHY

in

Biochemistry

Approved:

Scott A. Ensign, Ph.D.
Major Professor

Lance C. Seefeldt, Ph.D.
Committee Member

Joan M. Hevel, Ph.D.
Committee Member

John L. Hubbard, Ph.D.
Committee Member

Paul G. Wolf, Ph.D.
Committee Member

Mark R. McLellan, Ph.D.
Vice President for Research and
Dean of Graduate Studies and

UTAH STATE UNIVERSITY
Logan, Utah

2011

Copyright © Melissa A. Kofoed 2011

All Rights Reserved

ABSTRACT

Studies of the Distinguishing Features of NADPH:2-Ketopropyl-Coenzyme M
Oxidoreductase/Carboxylase, an Atypical Member of the Disulfide/
Oxidoreductase Family of Enzymes

by

Melissa A. Kofoed, Doctor of Philosophy

Utah State University, 2011

Major Professor: Dr. Scott Ensign
Department: Chemistry and Biochemistry

The metabolism of propylene in *Xanthobacter autotrophicus* occurs via epoxypropane formation and subsequent metabolism by a three-step, four-enzyme pathway, utilizing the atypical cofactor Coenzyme M (CoM) to form acetoacetate. The last step in the epoxide carboxylase pathway is catalyzed by a distinctive member of the disulfide oxidoreductase (DSOR) family of enzymes, NADPH:2-ketopropyl CoM oxidoreductase/carboxylase (2-KPCC). 2-KPCC catalyzes the unorthodox cleavage of a thioether bond and successive carboxylation of the substrate. The focus of the research presented in this dissertation aims to elucidate the details of 2-KPCC that allow it to perform chemistry unconventional for typical DSOR members. Site-directed mutagenesis was used to mutate specific active site residues and to examine the catalytic properties of 2-KPCC upon these changes. Mutation of His137, the proximal histidine that directly coordinates the water molecule, eliminated essentially

all redox-dependent activity of the enzyme while mutation of His84, the distal histidine that coordinates the water molecule through His137, diminished redox-dependent enzymatic activity to approximately 25% that of the wild type enzyme, confirming the respective roles of the histidine residues in stabilizing the enolate intermediate formed upon catalysis. Neither mutation of either histidine residue, nor mutation of either redox active cysteine residue had any negative effect on the rate of the redox-independent reaction catalyzed by 2-KPCC, the decarboxylation of acetoacetate. Mutation of Met140 resulted in an enzyme with drastically altered kinetic parameters and suggests Met140 plays a role in shielding the substrate from undesired electrostatic interactions with the surroundings.

The inhibitory properties of the structural CoM analogs, 2-bromoethanesulfonate (BES) and 3-bromopropanesulfonate (BPS), were examined and exploited to provide further detail on the active site microenvironment of 2-KPCC. Modification by BES results in a charge transfer complex between the thiolate of Cys87 and the oxidized flavin. The spectral features of this charge transfer complex have allowed the determination of the pK_a of the Cys87 to be significantly higher than the flavin thiol in other DSOR enzymes. BPS has been shown to be a competitive inhibitor of 2-KPCC with an inhibition constant over two orders of magnitude lower than for that of BES.

(107 pages)

ACKNOWLEDGMENTS

There are many people who have helped and supported me along my journey to obtain this degree and my sincerest gratitude to them cannot be adequately put into words.

First, I owe a great deal of thanks to my major professor, Scott Ensign, for his guidance and support over the past six years. His patience, thoughtfulness and encouragement have been of the utmost importance along the path of completing my degree. He has been an inspiration not only as a researcher, but as the kind of instructor that I aspire to be.

Second, I must thank my committee members, Dr. Seefeldt, Dr. Hevel and Dr. Hubbard, for their advice and suggestions and most importantly for their willingness to help whenever I may happen to drop by their office. Also, a big thank you to Dr. Wolf for his willingness to step in when a former committee member accepted a position at another university.

As I have spent the last year essentially alone in the lab, I am very aware of how tough lab life would have been without the companionship of my former lab mates and fellow graduate students. I am thankful for Dr. David Wampler for getting me started on my project and for helping me adjust to life here in Logan. I am also thankful for Dr. Laura Buelow (and Kris) for being my first friends after moving to Utah. My lab mates were instrumental in helping me maintain my sense of humor amid the struggles in the lab. Dr. Dariusz Sliwa, Ameya Mashruwala, Ashwini Wagh, and Brandon Russell, thank you so much for all of the laughs, birthday cake, practical jokes, and good conversations. I am also grateful for the friendship of all of

the graduate students within the department even though there are too many to mention all by name.

I never would have survived these past six years if it weren't for the support from my family and friends. I especially must thank my parents for all of their support throughout my life and through my decision to move to Utah and go to graduate school. I am also particularly grateful for my mother- and father-in-law and their willingness to help watch our little boy while I finished my degree. Although many states away, I owe so much to my sisters and friends, Kaydee, Elizabeth, Melissa, Casey, and Amanda, for their positive emails, phone calls, and visits.

And lastly, thank you to my husband, Tim, for all of your support and encouragement, including, but not limited to, bringing countless dinners up to the lab, driving to school with me in the middle of the night when I woke up in a panic thinking I had forgotten to do something, and for giving up skiing to stay home with Kelton on the weekends while I worked in the lab. Kelton, thank you for being my ray of sunshine on even the gloomiest days, and for making me aware that I am capable on functioning on even less sleep than I ever thought possible.

Missy (Beighley) Kofoed

CONTENTS

	Page
ABSTRACT	iii
ACKNOWLEDGMENTS	v
LIST OF TABLES	viii
LIST OF FIGURES	ix
ABBREVIATIONS	xi
CHAPTER	
1. INTRODUCTION	1
2. MECHANISTIC CHARACTERIZATION OF 2-KPCC BY CHARACTERIZATION OF H137A, H84A AND M140A SITE DIRECTED MUTANTS	29
3. COMPLETED STUDIES OF C87A and C82A 2-KPCC AND COMPARATIVE SPECTRAL ANALYSIS OF C82A AND 2- BROMOETHANESULFONATE MODIFIED 2-KPCC	51
4. BROMOPROPANESULFONATE AS AN INHIBITOR OF GROWTH IN <i>XANTHOBACTER AUTOTROPHICUS</i> AND AN INHIBITOR AND SELECTIVE ALKYLATING AGENT OF 2-KPCC	69
5. CONCLUSIONS AND FUTURE DIRECTIONS	86
APPENDIX	91
CURRICULUM VITAE	93

LIST OF TABLES

Table		Page
2-1	Redox-dependent activities of wild type, H84A and H137A 2-KPCC	39
2-2	Comparison of kinetic parameters between wild type and M140A 2-KPCC	45

LIST OF FIGURES

Figure	Page
1-1	Biological strategies of epoxide degradation/metabolism 3
1-2	Pathway of propylene metabolism in <i>X. autotrophicus</i> strain Py2.....6
1-3	Structure of 2-mercaptoethanesulfonate (Coenzyme M).....7
1-4	Proposed mechanism for EaCoMT, utilizing zinc to activate the thiol of CoM for nucleophilic attack on epoxypropane.....9
1-5	Proposed mechanism of reductive cleavage and subsequent carboxylation or protonation of the enolacetone intermediate formed as catalyzed by 2-KPCC.....11
1-6	Reactions catalyzed by 2-KPCC15
1-7	Catalytic triad in the active site of 2-KPCC formed by His84, His137, and an ordered water molecule that serves to stabilize the enolate intermediate formed upon catalysis16
1-8	Comparison of the mixed disulfide state of 2-KPCC, with 2-KPCC modified by BES and BPS19
2-1	Schematic representation illustrating the fate of the enolate intermediate formed upon attack of the CoM thiol by Cys82 of 2-KPCC, which can undergo carboxylation, or in the absence of CO ₂ , protonation.....31
2-2	Active site of 2-KPCC with the substrate, 2-KPC bound.....33
2-3	Time course of acetone production as a product of 2-KPCC catalyzed acetoacetate decarboxylation41
2-4	Active site of 2-KPCC showing the position of 2-KPC where the sulfonate is oriented by Arg56 and Arg36543
2-5	Initial velocities of 2-KPC cleavage and carboxylation to form acetoacetate as a function of [2-KPC].....44
3-1	Active site of 2-KPCC with substrate bound.....53

3-2	Acetone production as a result of 2-KPCC catalyzed acetoacetate decarboxylation.....	60
3-3	UV-visible spectra of untreated 2-KPCC and BES-modified 2-KPCC.....	61
3-4	UV-visible spectra of BES modified 2-KPCC at varying pH showing the development of spectral charge transfer characteristics as a function of increasing pH.....	62
3-5	Determination of the pK_a of Cys87.....	63
3-6	Comparison of the active sites of 2-KPCC and glutathione reductase.....	64
4-1	Comparative structures of 2-mercaptoethanesulfonate (CoM), 2-bromoethanesulfonate (BES) and 2-bromopropanesulfonate (BPS).....	72
4-2	Growth of <i>X. autotrophicus</i> in the presence and absence of BPS.....	77
4-3	Competitive rapid equilibrium inhibition of 2-KPCC catalyzed 2-KPC oxidation by BPS.....	79
4-4	Spectral changes associated upon modification of 2-KPCC that had been alkylated by BPS.....	80
4-5	Comparison of the mixed disulfide formed in 2-KPCC during catalysis between the interchange thiol and the thiol of CoM and 2-KPCC that had been alkylated by BES or BPS at Cys82.....	82

ABBREVIATIONS

2-KPC	2-ketopropyl CoM
2-KPCC	NADPH:2-ketopropyl Coenzyme M oxidoreductase/carboxylase
λ_{\max}	wavelength maximum
A_{340}	absorbance at 340 nm
A_{450}	absorbance at 450 nm
A_{555}	absorbance at 555 nm
Arg	arginine
β -HBDH	β -hydroxybutyrate dehydrogenase
BES	2-bromoethanesulfonate
BPS	3-bromopropanesulfonate
CoM	Coenzyme M (2-mercaptoethanesulfonate)
CoB	Coenzyme B
Cys	cysteine
DSOR	NAD(P)H disulfide oxidoreductase
DTT	dithiothreitol
ϵ_{450}	extinction coefficient at 450 nm
EaCoMT	epoxyalkane:CoM transferase
EDTA	ethylenediaminetetraacetic acid
FAD	oxidized flavin adenine dinucleotide
Gln	glutamine
GSH	glutathione

GTP	glycine-tris-phosphate
h	hours
His	histidine
HPC	hydroxypropyl CoM
K_a	acid dissociation constant
k_{cat}	turnover number
K_i	inhibition constant
K_m	Michaelis constant
LB-Rich	Luria-Bertani
MCR	methyl-CoM reductase
Met	Methionine
NAD^+	oxidized nicotinamide adenine dinucleotide
NADH	reduced nicotinamide adenine dinucleotide
$NADP^+$	oxidized nicotinamide adenine dinucleotide phosphate
NADPH	reduced nicotinamide adenine dinucleotide phosphate
NMR	nuclear magnetic resonance
OD_{600}	optical density at 600 nm
Phe	phenylalanine
psi	pounds per square inch
R_f	retention factor
RCF	relative centrifugal force
R-HPC	R-hydroxypropyl CoM

R-HPCDH	R-hydroxypropyl CoM dehydrogenase
rpm	rotations per minute
SDR	short chain dehydrogenase/reductase
SDS-PAGE	sodium dodecyl sulfate polyacrylamide gel electrophoresis
S-HPC	S-hydroxypropyl CoM
S-HPCDH	S-hydroxypropyl CoM dehydrogenase
TPP	thiamin pyrophosphate
Tris	tris(hydroxymethyl)aminomethane
UV-Vis	ultraviolet-visible spectroscopy
v/v	volume/volume
V _{max}	theoretical maximum reaction rate

CHAPTER 1

INTRODUCTION

Background and Significance

The increased economic growth and development of our global community has created an increased dependency on industrial processes resulting in increased atmospheric concentrations of not only typical greenhouse gases like CO and CO₂, but of a variety of environmentally detrimental gaseous hydrocarbons. Of particular interest, are short chain alkenes and their halogenated equivalents. The corresponding epoxides formed from them are especially toxic due to their highly electrophilic nature and propensity to react with cellular proteins and DNA to form covalent adducts (51). The increased concentrations of these compounds not only impart a serious risk to human health but also threaten to destabilize our ecosystems through a wide variety of mechanisms. Interestingly, several bacteria have been identified that are able not only to detoxify short chain aliphatic alkenes, but are able to convert them to non-reactive central metabolites while fixing a molecule of CO₂ in the process (19). *Xanthobacter autotrophicus* strain Py2 is one such bacteria, isolated with propylene, and capable of growth on the corresponding epoxide, epoxypropane (2). Additionally, *X. autotrophicus* strain Py2 can also grow using other short chain hydrocarbons such as ethylene, 1-butylene, 2-butylene, 1-pentene and 1-hexene (49, 50). While there is clearly an interest in these organisms with regards to bioremediation, it is also of importance to understand the fundamental mechanisms used by the bacteria rendering them capable of metabolizing and detoxifying xenobiotics.

The research presented in this dissertation aims to further the understanding of the method and mechanism used by *X. autotrophicus* to detoxify and metabolize epoxides, with particular focus on the details of the CoM regenerating, terminal enzyme in the pathway, a novel member of the disulfide oxidoreductase (DSOR) family of enzymes that is also a carboxylase.

Sources of Propylene and Epoxides.

Propylene is produced as a byproduct in the refining process of petroleum and natural gas. Epoxypropane, also known as propylene oxide, generated from propylene, is used in its gaseous form as a sterilant in hospitals and in its liquid form as an additive to increase the effectiveness of disinfectant solutions (25). Epoxypropane is also produced biogenically from alkenes in a variety of organisms as the first step in either the detoxification of alkenes, or the utilization of alkenes as a primary energy source by broad specificity monooxygenases, including cytochrome P-450 enzymes in plants and animals (23), and an alkene monooxygenase in the bacteria *X. autotrophicus* strain Py2 and *Rhodococcus rhodochrous* (2, 3).

Biological Strategies of Epoxide Detoxification.

There are two basic strategies organisms utilize to undermine the potentially toxic effects of epoxides within the cell, 1) conversion to detoxification products or 2) productive metabolism allowing the epoxides formed to be utilized as a primary carbon and energy source. The majority of organisms are not capable of using alkenes or the corresponding epoxides as primary energy sources and instead possess detoxification enzymes that allow the conversion of epoxides to less toxic products, most commonly

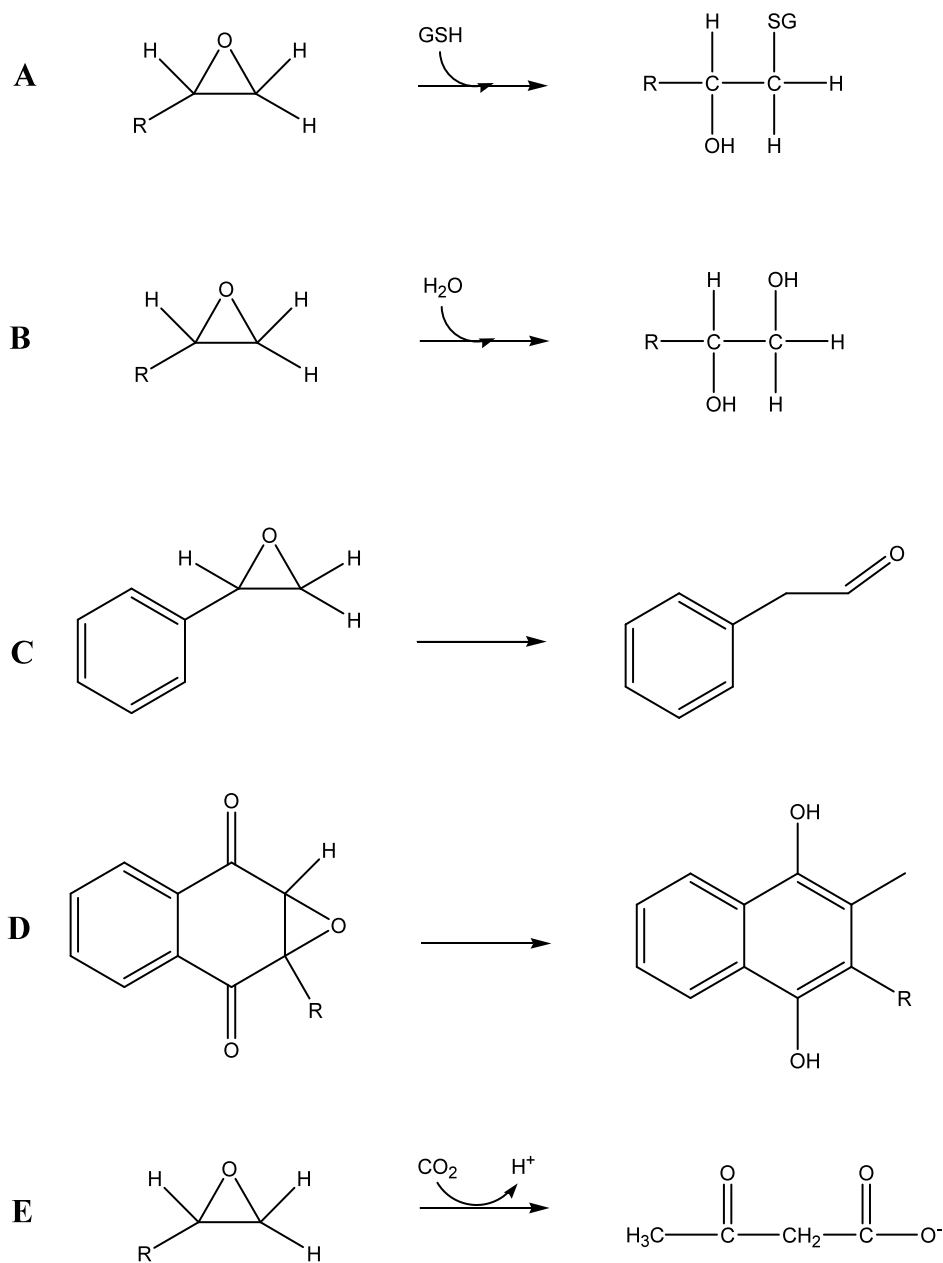


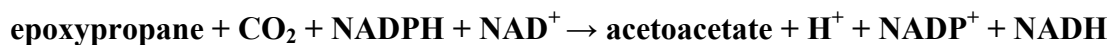
Figure 1-1. Biological strategies of epoxide degradation/metabolism. Examples of enzymes which utilize such strategies: A, glutathione transferase; B, epoxide hydrolase; C, styrene oxide isomerase; D, vitamin K epoxide reductase; E, epoxyalkane:CoM transferase.

glutathione S-transferases (6, 43). Glutathione S-transferases catalyze the opening of the epoxide ring with concomitant glutathione conjugation as shown in Figure 1-1. There is also an enzyme used in the vitamin K cycle, vitamin K epoxide reductase, which functions to regenerate the dihydroquinone form of vitamin K for use by vitamin K carboxylase (52, 53). Bacteria that can productively metabolize epoxides employ several different methods, including hydration of the epoxide by an epoxide hydrolase in bacteria capable of growth on epoxypropane or epichlorohydrin (7, 27) or isomerization of the epoxide to the corresponding aldehyde in the case of bacteria capable of growth on styrene (42). The most unconventional of these methods involves carboxylation of the epoxide to a β -keto acid as described below.

Propylene Metabolism via Epoxypropane Formation in *X. autotrophicus* strain Py2.

Propylene metabolism in *X. autotrophicus* strain Py2 proceeds by insertion of oxygen across the olefin bond forming the corresponding epoxides in a stereospecific manner by an alkene monooxygenase (46) with R-epoxypropane being formed in 95% enantiomeric excess (1). This alkene monooxygenase is a four component enzyme, consisting of a hexameric epoxygenase that contains four mol of nonheme iron, a reductase that contains FAD and a 2Fe-2S cluster, a homodimeric ferredoxin containing two Rieske-type 2Fe-2S clusters and an effector protein with an as yet to be determined function (46).

Epoxides are not only detoxified but also converted to the more easily assimilated metabolite acetoacetate by a three step, four enzyme pathway which catalyzes the carboxylation of epoxypropane according to the following overall equation (4):



The novelty of this pathway includes the use of an atypical cofactor thought previously to function only in methanogenic archaea, the presence of a pair of short chain dehydrogenase enantiomers which catalyze the same reaction but with opposite stereospecificity, as well as an innovative strategy of substrate carboxylation (Figure 1-2) (1, 5, 14).

History of Coenzyme M.

Coenzyme M (2-mercaptoethanesulfonic acid) was first discovered in the laboratory of Ralph Wolfe in 1971, as a cofactor involved in methanogenic archaea as a methyl group carrier during key reactions involved in the production of methane (36, 47, 56). In addition to being the smallest organic cofactor known to date, it is also the only presently known cofactor containing a sulfonic acid functional group (Figure 1-3). It is the unprecedented sulfonate group of CoM that plays a key role in substrate recognition of the enzymes in the epoxide carboxylase pathway.

Methyl-Coenzyme M Reductase. There are several pathways for methane production utilizing various substrates, but all converge with the common intermediate, methyl-CoM (48, 56). The enzyme responsible for the final step in these pathways, methyl-CoM reductase (MCR), catalyzes a heterodisulfide bond formation between methyl-CoM and Coenzyme B (CoM-S-S-CoB), releasing methane in the process. The active site of MCR facilitates this chemistry by using a nickel tetrapyrrole cofactor, F₄₃₀ (17, 18, 20, 55). There are currently two mechanisms that have been proposed for MCR, the first, which proceeds by attack of Ni(I) on the methyl group of CoM forming a

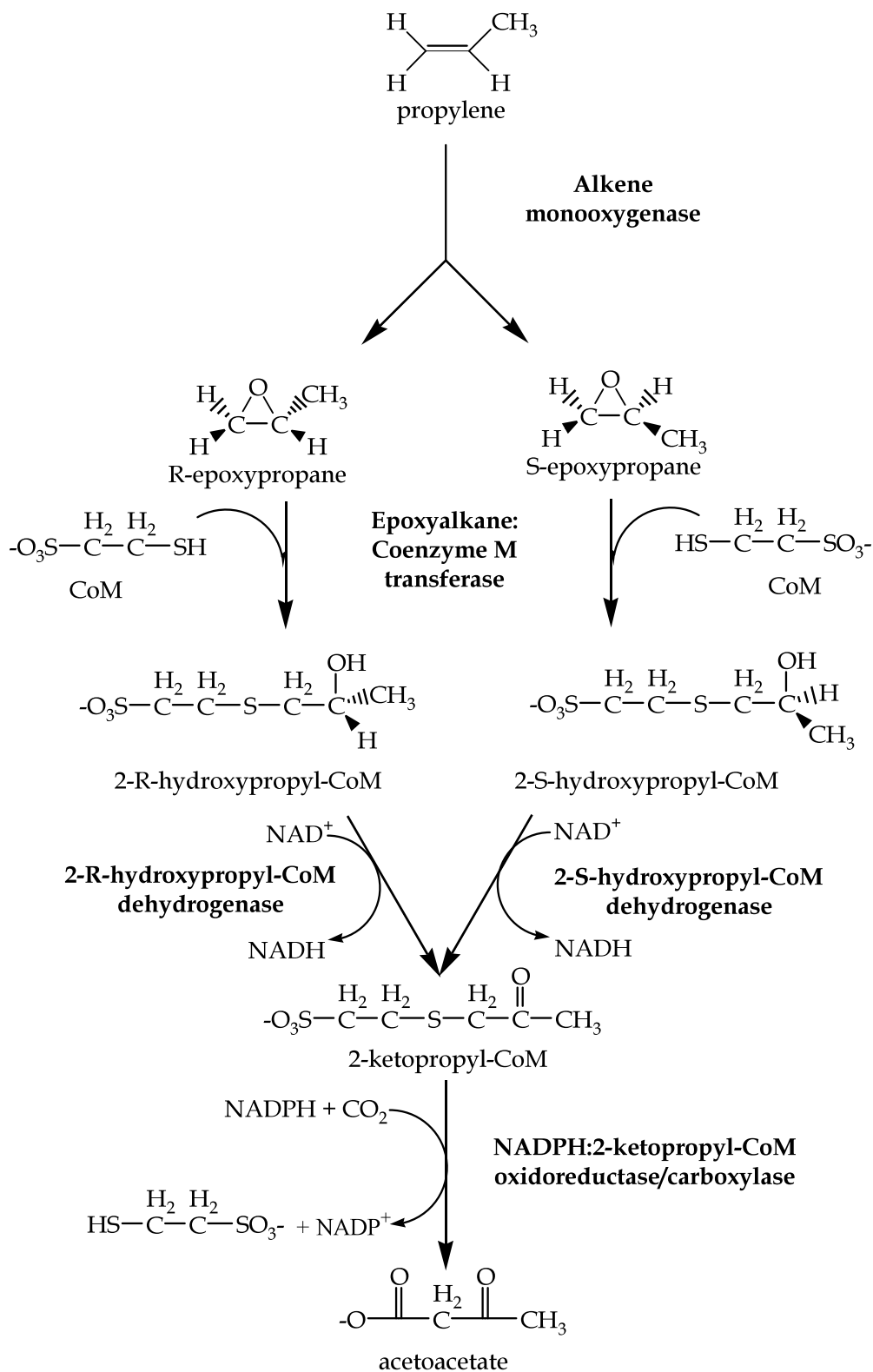


Figure 1-2. Pathway of propylene metabolism in *X. autotrophicus* strain Py2.

methyl-Ni(III) intermediate, and the second, which proceeds by attack of Ni(I) on the thioether sulfur of CoM resulting in a Ni(II)-S-CoM intermediate (33). Although the details of the mechanistic intermediates remain to be elucidated, the products of the reaction are methane and CoM-S-S-CoB. The reduction of the disulfide bond formed between CoM and CoB is subsequently reduced by a heterodisulfide reductase, generating free CoM and CoB and allowing the coenzymes to be recycled for further use in metabolic pathways (26).

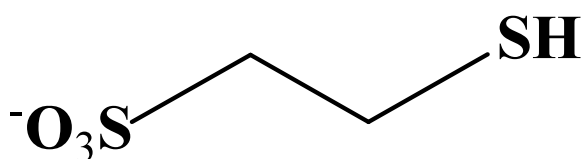


Figure 1-3. Structure of 2-mercaptoethanesulfonate (Coenzyme M).

A Role for Coenzyme M Outside of Methanogens. The use of CoM in bacterial hydrocarbon metabolism wasn't discovered until close to thirty years later in the laboratory of Scott Ensign (1). Upon investigating the metabolic pathway of epoxide metabolism in *X. autotrophicus* strain Py2, an unknown nucleophilic cofactor was found to co-purify with epoxyalkane:CoM transferase, then known as Component I. Incubation of radiolabeled epoxypropane with purified Component I resulted in Component I, which when separated from small molecules by gel filtration, retained no catalytic activity. A small radiolabeled compound was then isolated from the gel filtration eluent, which when analyzed by NMR, was found to have the structure of ring opened epoxypropane

covalently bound to CoM. Additional studies found that the CoM molecule serves as a nucleophile involved in opening of the epoxide ring and subsequently as a carrier for the various intermediate products in the epoxide degradation pathway (14, 16, 32). The sulfonate moiety of CoM serves to orient the substrates in the active sites of their respective enzymes by the presence of either two arginine residues, or an arginine and lysine residue present in the active site (15, 30, 38). In the final step in the pathway, CoM is cleaved from 2-ketopropyl-CoM (2-KPC) by the action of NADPH:2-ketopropyl-CoM oxidoreductase/carboxylase (2-KPCC), allowing the free CoM molecule to be recycled for further cycles in the pathway.

Epoxyalkane:CoM Transferase

The first step in the epoxide degradation pathway in *X. autotrophicus* is catalyzed by epoxyalkane:CoM transferase (EaCoMT), a hexameric protein containing 1 Zn per subunit (31). EaCoMT catalyzes the addition of CoM to either *R*- or *S*-epoxypropane and concomitant opening of the epoxide ring, forming *R*- or *S*-hydroxypropyl-CoM respectively (*R*-HPC, *S*-HPC). Primary sequence analysis of EaCoMT has shown that it belongs to a family of alkyl transferases that utilize zinc to activate a thiol for nucleophilic attack, such as methionine synthase (57). However, EaCoMT differs from other members of this family in that it catalyzes a nucleophilic addition rather than a nucleophilic substitution (Figure 1-4). Evidence has been shown that the role of the zinc ion in the active site of EaCoMT is to bind CoM and to lower the pK_a of the thiol from 9.1 to 7.4, activating CoM for nucleophilic attack on epoxypropane (13, 31). In addition to lowering the pK_a of the thiol, analysis using isothermal titration calorimetry concluded that the zinc-thiol interaction contributes to over half of the total binding energy (31).

R- and S-hydroxypropyl-CoM Dehydrogenases

Both *R*- and *S*-hydroxypropyl-CoM are converted to a common intermediate, 2-ketopropyl-CoM (2-KPC), by the action of two stereospecific short chain dehydrogenases/reductases (SDR) (28). Currently, among the SDR family, there is only one other known pair of enzymes, other than the bacterial HPC dehydrogenases, which catalyze the same reaction but with opposite stereospecificity, a pair of plant tropinone reductases (37).

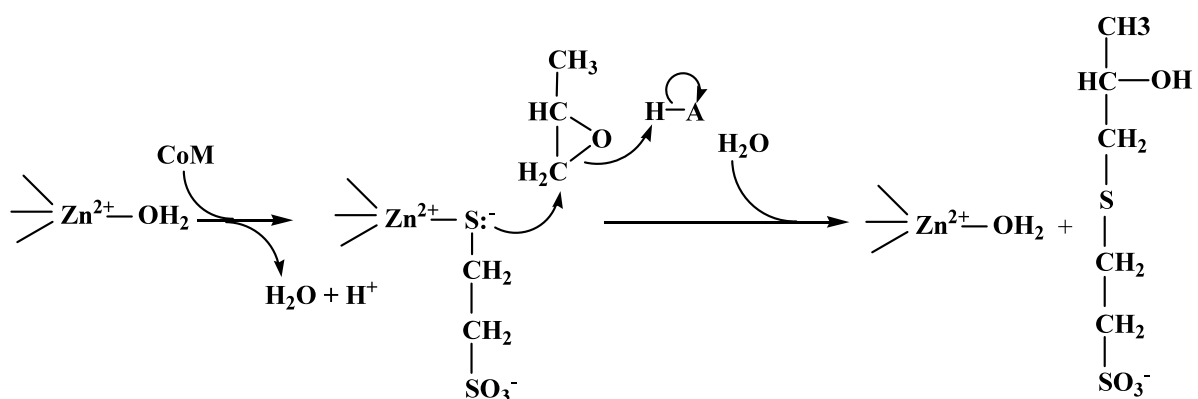


Figure 1-4. Proposed mechanism for EaCoMT, utilizing zinc to activate the thiol of CoM for nucleophilic attack on epoxypropene.

As typical for SDR enzymes, *R*- and *S*-HPCDH, are NAD⁺ dependent enzymes with a conserved catalytic triad consisting typically of a serine, tyrosine and lysine residue (28). A general mechanism has been proposed for SDR enzymes, where the deprotonated tyrosine residue serves as a general base for abstraction of a proton from the

substrate molecule. The lysine residue serves to bind the sugar moiety of NAD^+ and to stabilize the deprotonated tyrosine. The serine residue in the conserved catalytic triad functions to increase the acidity of the substrate hydroxyl group through hydrogen bonding and to stabilize the developing charge on the alcohol oxygen in the transition state.

Of significant interest is that while both enzymes are highly discriminating for their corresponding substrate, *R*-HPCDH and *S*-HPCDH have entirely different mechanisms of substrate specificity. As previously stated, *R*-epoxypropane is formed in greater than 95% enantiomeric excess. Although *S*-epoxypropane is a minor metabolic product, it is still necessary for the organism to metabolize this otherwise toxic epoxide. If *S*-epoxypropane were converted only to *S*-HPC by the action of EaCoMT, CoM would be sequestered in the molecule and unable to be regenerated for reuse within the pathway. Thus, the specificity of these dehydrogenases have evolved in such a way as to deal with the efficient substrate flux through the pathway of *R*- and *S*-epoxypropane, and by extrapolation, *R*- and *S*-HPC formed. Previous studies have shown that *R*-HPCDH exhibits selectivity by catalyzing oxidation of the opposite enantiomer (*S*-HPC) with a 402 times lower k_{cat} , while *S*-HPCDH exhibits selectivity by catalyzing *R*-HPC oxidation with a K_m 209 times higher than that for *S*-HPC (45).

NADPH:2-Ketopropyl-CoM Oxidoreductase/Carboxylase.

The final step in this pathway, and the main focus of the research in this dissertation, is catalyzed by NADPH:2-ketopropyl-CoM oxidoreductase/carboxylase (2-KPCC). 2-KPCC, formerly known as Component II, is a member of the disulfide oxidoreductase (DSOR) family of enzymes, whose members include glutathione

reductase, thioredoxin reductase and lipoamide dehydrogenase (8, 35, 41). 2-KPCC reductively cleaves and carboxylates 2-KPC, yielding acetoacetate and regenerating the CoM cofactor. As typical of DSOR enzymes, 2-KPCC utilizes the non-covalently bound cofactor FAD. Electrons are transferred from NADPH to FAD⁺, which then reduces the internal disulfide bond between two conserved cysteine residues, referred to, with respect to the flavin, as the proximal and interchange thiols (21). Reduction of the disulfide

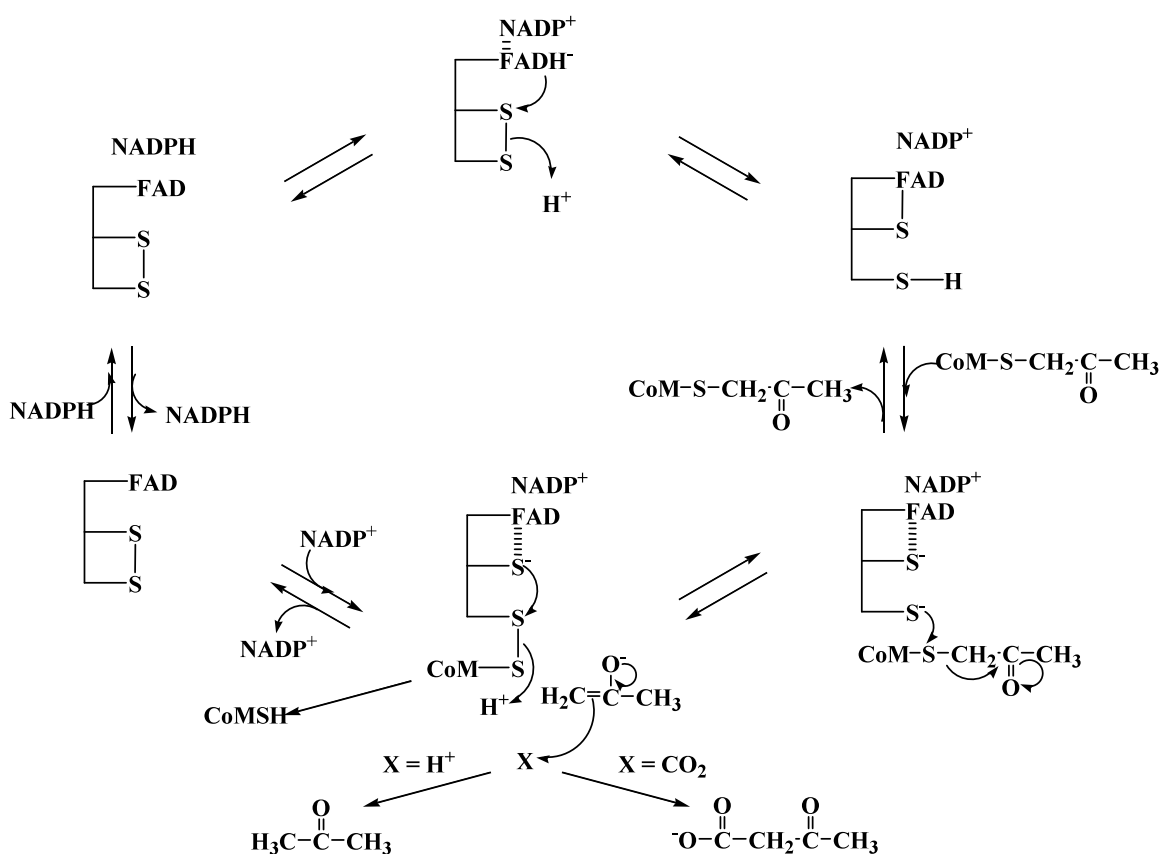


Figure 1-5. Proposed mechanism of reductive cleavage and subsequent carboxylation or protonation of the enolacetone intermediate formed as catalyzed by 2-KPCC. This figure was adapted from Clark and Ensign (14).

allows for nucleophilic attack by the interchange thiol on the sulfur atom of CoM, forming a mixed disulfide between the interchange thiol and CoM and generating the enolate of acetone as seen in Figure 1-5. The enolate of acetone can then be either protonated or carboxylated, allowing reformation of the internal disulfide bond and releasing free CoM.

DSOR Family of Enzymes.

Typical features of DSOR enzymes include the transfer of a hydride from NAD(P)H to FAD and subsequent transfer of electrons from FADH to reduce a redox active disulfide in the active site of the enzyme. The free thiols are designated the proximal, or flavin, thiol and the distal, or interchange thiol. Canonical members of the DSOR family such as glutathione reductase, thioredoxin reductase and lipoamide dehydrogenase catalyze disulfide bond cleavage resulting initially in a mixed disulfide formed between the interchange thiol and the substrate molecule (9, 29, 35, 54). This is followed by reduction and subsequent release of the bound substrate with reformation of the active site cysteine disulfide.

As flavin containing enzymes, DSOR enzymes exhibit a variety of spectral features and studies of the changes of these features have often provided considerable insight into the attributes and mechanisms of these enzymes.

In the fully oxidized form, with respect to both the flavin and disulfide, DSOR enzymes exhibit absorption maxima at approximately 365 nm and 450 nm, which are both bleached upon four-electron reduction. Although a variety of techniques have been utilized to examine spectral changes in DSOR enzymes, including stopped flow

spectroscopy, site directed mutagenesis of the interchange cysteine with a non-thiol containing residue has proven to be considerably advantageous.

Upon mutation of the interchange thiol to alanine, a flavin-thiolate charge transfer absorbance can be observed. Because this charge transfer is only observed when the proximal thiol is in the unprotonated thiolate form, base titration of the oxidized enzyme can provide considerable insight into the pK_a of the flavin thiol and hence the microenvironment of the enzyme active site. The pK_a values for the proximal cysteine in glutathione reductase and mercuric ion reductase have been determined to be 4.8 and 5.2 (9, 44), respectively which differs significantly from the pK_a value of 8 for free cysteine and is thought to be predominantly the result of the presence of a catalytically essential conserved histidine residue within the active site of the enzyme.

Novel Features of 2-KPCC.

Although the general mechanism is the same, 2-KPCC is unique to the DSOR family of enzymes in many ways, with the most significant difference being the catalysis of thioether bond cleavage (as opposed to disulfide bond cleavage) and subsequent carboxylation of the substrate.

Whereas reductive cleavage and carboxylation of the substrate is the primary physiologically relevant reaction catalyzed, 2-KPCC is also capable of protonating the enolacetone formed during catalysis in the absence of $\text{CO}_2/\text{HCO}_3^-$ as well as catalyzing the reverse reaction, the formation of 2-KPC from acetoacetate and CoM (14) as seen in Figure 1-6abc. In addition to the redox dependent reactions, 2-KPCC is also capable of two redox independent reactions, acetoacetate decarboxylation to form acetone and CO_2

and acetoacetate/ $^{14}\text{C}\text{O}_2$ exchange to form $^{14}\text{C}_1$ -acetoacetate and CO_2 (14) as seen in Figure 1-6de.

Although enzyme catalysis of thioether bond cleavage may seem unlikely, previous studies have been done where the flavin thiol was mutated to an alanine residue. Unable to reform a disulfide bond, the interchange thiol remained in reduced state. Incubation of this variant 2-KPCC with the physiological substrate produced 0.76 moles of product per mol of enzyme active site (Wampler, unpublished). Incapable of regenerating a disulfide bond, CoM most likely remained bound to the interchange thiol and rendered the enzyme incapable of catalyzing more than a single turnover. Structural studies have also provided evidence for a mixed-disulfide intermediate (40).

Also setting 2-KPCC apart from typical DSOR members are differences in active site location and composition. In glutathione reductase, as well as most DSOR members, the active site and redox active disulfide are located at the base of a large open cleft (6). In addition to providing for easy substrate access and product release, an open access site provides access to protons from the bulk solvent, which is favorable as most DSOR enzymes catalyze the reductive cleavage and protonation of their respective substrates. As 2-KPCC preferentially catalyzes carboxylation versus protonation of the substrate, unlimited access of the active site to solvent would facilitate the formation of an unwanted side reaction. As such, 2-KPCC has marked differences in both the C- and N-termini of the protein as well as a thirteen amino acid loop insertion, which essentially block the open binding cleft. Instead, substrate access to the active site is limited to a well-defined channel, which collapses upon substrate binding (38). This collapse limits

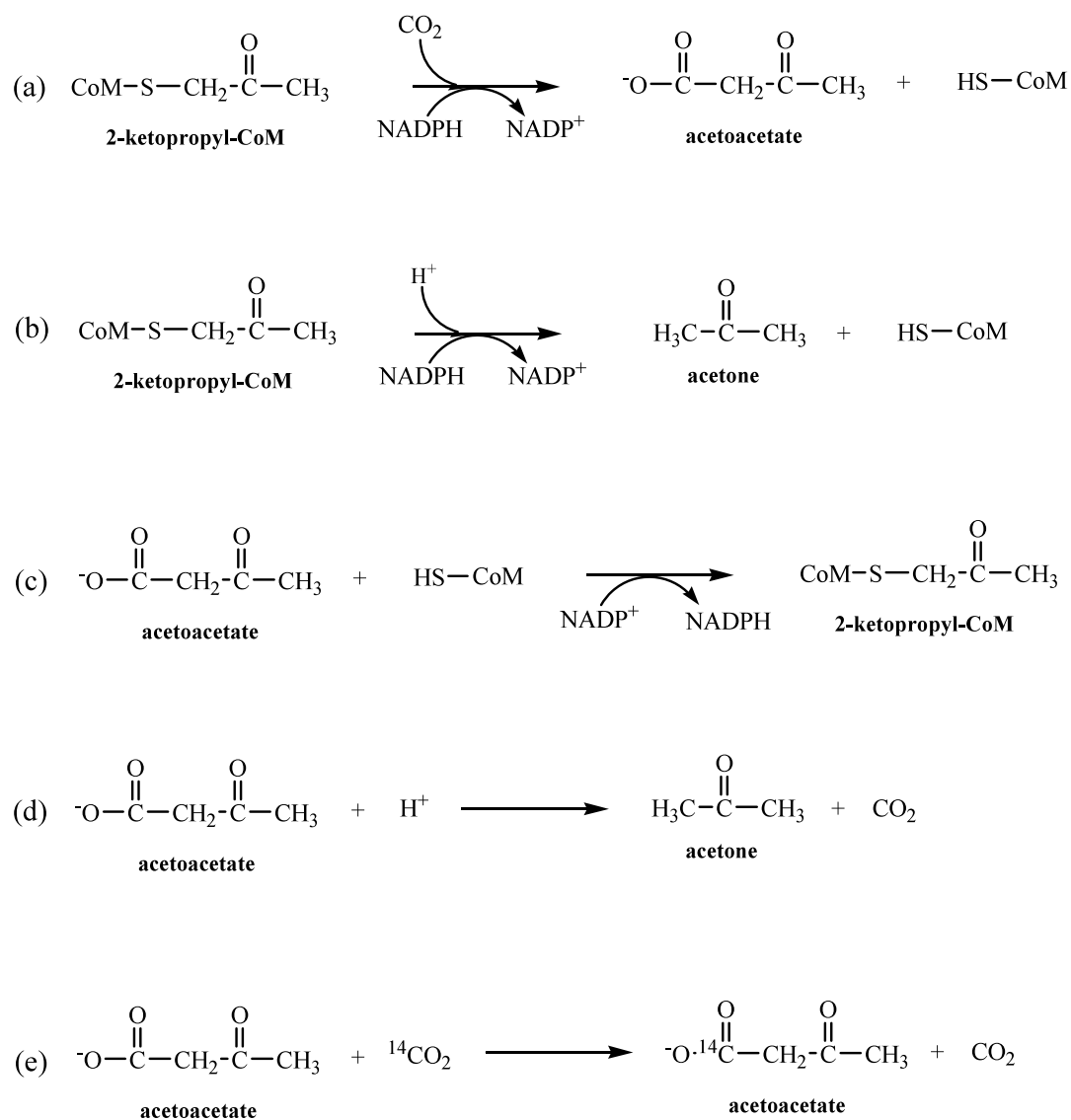


Figure 1-6. Reactions catalyzed by 2-KPCC. (a) reductive cleavage and carboxylation of 2-KPC forming acetoacetate and CoM; (b) reductive cleavage and protonation of 2-KPC forming acetone and CoM; (c) formation of 2-KPC from acetoacetate and CoM; (d) decarboxylation of acetoacetate; (e) CO₂ exchange.

access to the active site to a narrow hydrophobic channel, which allows access to CO₂ while discriminating against proton access.

Along with a buried active site, 2-KPCC also differs in that the active site is highly hydrophobic with the exception of a lone, ordered water molecule as evidenced by

a crystal structure solved with substrate bound (38). Unique to 2-KPCC, this water molecule is ordered by the presence of two histidine residues, one which coordinates the water molecule directly (His137) and one, which coordinates the water molecule indirectly through His137 (His 84). The presence of this “catalytic triad” serves to stabilize the enolate intermediate formed during catalysis and is supported by both biochemical and structural studies (39).

Structural studies have indicated that upon catalysis and product release, the imidazole ring of His137 is rotated 180° away from the active site cavity and that the water molecule previously bound to His137 migrates to within hydrogen-bonding distance of the thiol of CoM (40). Because there are no charged residues in the active site

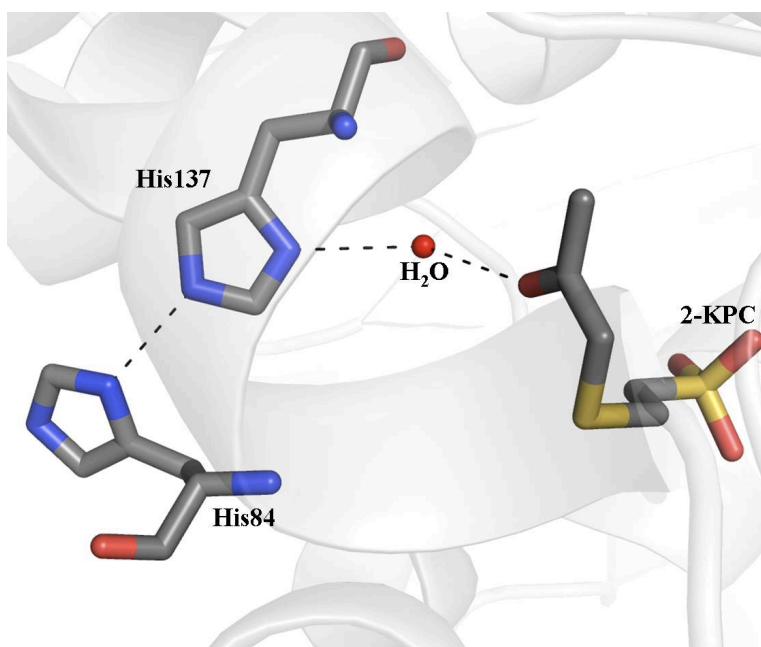


Figure 1-7. Catalytic triad in the active site of 2-KPCC formed by His84, His137 and an ordered water molecule that serves to stabilize the enolate intermediate formed upon catalysis.

of 2-KPCC that are in close enough proximity of the enzyme-CoM mixed disulfide to facilitate an attack and release CoM, it is hypothesized that the water molecule might be fulfilling this role. It is important to note that this water molecule is ordered by His137 until after carboxylation of the substrate and dissociation of the acetoacetate formed, helping to further promote carboxylation over protonation of the substrate.

The contrasting active site of 2-KPCC is further distinguished by the significantly higher pK_a of the flavin cysteine residue. Two different methods, site directed mutagenesis of the interchange cysteine and modification of the interchange cysteine by alkylation both gave the same pK_a value for the flavin cysteine residue of approximately 8.75, which is considerably higher than the pK_a values determined for those typical DSOR members such as glutathione reductase. In typical DSOR enzymes, there is also a conserved histidine residue which in 2-KPCC is replaced by a phenylalanine residue, most likely to preserve the hydrophobicity of the active site and which is believed to be at least partly responsible for the increase in the pK_a of the flavin thiol.

Bromoethanesulfonate and Bromopropanesulfonate as Inhibitors of CoM-dependent pathways.

2-bromoethanesulfonate (BES) was first identified as a potent inhibitor of methanogenesis when certain preparations of methyl-CoM, which utilized BES as a starting compound for synthesis, would not serve as a substrate for the methylreductase reaction (10). BES inhibits methanogenesis by specifically inactivating methyl-CoM reductase by oxidation of the Ni(I) in the nickel tetrapyrrole cofactor F_{430} to Ni(II) (22).

3-bromopropanesulfonate (BPS) is an even more potent inhibitor of methanogenesis than BES, however, although it also oxidizes the Ni(I), it does so by a different mechanism, forming an alkyl-Ni(III) intermediate (34).

As expected, both of the structural CoM analogs, BES and BPS, have been shown to be inhibitors of the epoxide carboxylase pathway and inhibit growth of *X. autotrophicus* strain Py2 on propylene, but not with carbon sources that do not utilize the CoM-dependent pathway (11). Concentrations of lower than 1 mM BES had no effect on bacteria growth, while BES completely inhibits growth of the bacteria at a concentration of 3 mM. It is interesting to note that the threshold concentration of BES required for complete growth inhibition of *X. autotrophicus* is significantly lower than the 0.44 to 10 μ M BES concentration required for complete growth inhibition in methanogens (11, 24).

BES has been shown to be a reversible rapid equilibrium inhibitor of enzymes involved in the last two steps in the epoxide degradation pathway, R-HPCDH and 2-KPCC, as well as a time dependent irreversible inactivator of 2-KPCC (12). The mechanism of 2-KPCC inactivation by BES is unprecedented for a CoM-dependent enzyme and occurs by the specific irreversible alkylation of the interchange thiol. Like CoM and CoM containing substrates, BES is oriented in the active sites of the previously mentioned enzymes by interaction of the sulfonate group of the molecule with two positively charged arginine residues conserved between the enzymes. Alkylation of 2-KPCC likely occurs by attack of the interchange thiol on BES according to the mechanism in Figure 1-8.

Intriguingly, BES is not an inhibitor of EaCoMT, which is the only enzyme in the epoxide carboxylase pathway for which CoM is a substrate. As previously mentioned,

and in contrast to the other enzymes in the pathway, binding of CoM to EaCoMT is dictated largely by the zinc-thiol interaction and not the interaction of the protein with the

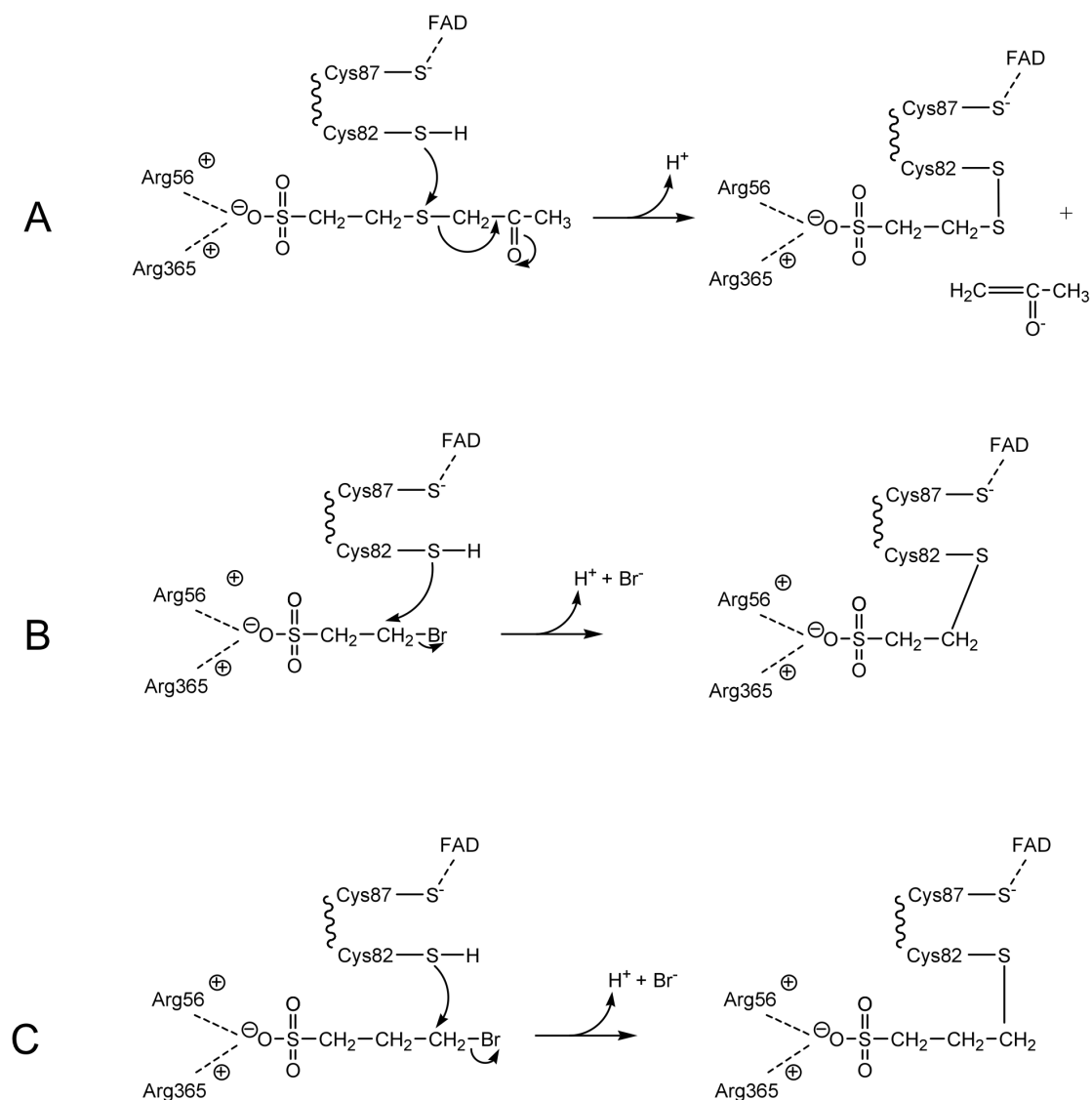


Figure 1-8. Comparison of the mixed disulfide state of 2-KPCC, with 2-KPCC modified by BES and BPS. A, Mixed disulfide formed between the interchange thiol of 2-KPCC and the thiol of CoM during catalysis; B, alkylation of the interchange thiol of 2-KPCC by BES; C, alkylation of the interchange thiol of 2-KPCC by BPS.

sulfonate group (31). Therefore, the absence of a thiol in BES results in the loss of a key interaction between this molecule and the protein making it a poor CoM analog and inhibitor for EaCoMT. From this reasoning, it is rational to assume that BPS would also be an unlikely inhibitor of EaCoMT.

In contrast to the concentration of BES required for growth inhibition in *X. autotrophicus*, BPS inhibits growth at concentrations over two orders of magnitude lower. The increased toxicity of BPS as compared to BES is likely due to the increased length of the BPS molecule making it a better CoM mimic after alkylation to the interchange thiol (Figure 1-8), placing it in a better orientation in the active site for attack from the interchange thiol.

Concluding Remarks.

The research presented in this dissertation attempts to further the understanding of an unprecedented member of the DSOR family and the novel features that make it ideal for the role it plays as the terminal enzyme in aliphatic epoxide carboxylation. The details of epoxide carboxylation as well as highlights of methanogenesis were discussed in order to provide context and background as well as to accentuate the importance and novelty of the method of epoxide detoxification by *X. autotrophicus* strain Py2, including the use of the atypical cofactor, coenzyme M.

REFERENCES

1. **Allen, J. R., D. D. Clark, J. G. Krum, and S. A. Ensign.** 1999. A role for coenzyme M (2-mercaptoethanesulfonic acid) in a bacterial pathway of aliphatic epoxide carboxylation. *Proc. Natl. Acad. Sci. USA* **96**:8432-8437.
2. **Allen, J. R., and S. A. Ensign.** 1996. Carboxylation of epoxides to β -keto acids in cell extracts of *Xanthobacter* strain Py2. *J. Bacteriol.* **178**:1469-1472.
3. **Allen, J. R., and S. A. Ensign.** 1998. Identification and characterization of epoxide carboxylase activity in cell extracts of *Nocardia corallina* B276. *J. Bacteriol.* **180**:2072-2078.
4. **Allen, J. R., and S. A. Ensign.** 1997. Purification to homogeneity and reconstitution of the individual components of the epoxide carboxylase multiprotein enzyme complex from *Xanthobacter* strain Py2. *J. Biol. Chem.* **272**:32121-32128.
5. **Allen, J. R., and S. A. Ensign.** 1999. Two short-chain dehydrogenases confer stereoselectivity for enantiomers of epoxypropane in the multiprotein epoxide carboxylating systems of *Xanthobacter* strain Py2 and *Nocardia corallina* B276. *Biochemistry* **38**:247-256.
6. **Armstrong, R. N.** 1997. Structure, catalytic mechanism and evolution of the glutathione transferases. *Chem. Res. Toxicol.* **10**:2-18.
7. **Armstrong, R. N., and C. S. Cassidy.** 2000. New structural and chemical insights into the catalytic mechanism of epoxide hydrolases. *Drug Metab. Rev.* **32**:327-338.

8. **Arscott, L. D., S. Gromer, R. H. Schirmer, K. Becker, and C. H. Williams Jr.** 1997. The mechanism of thioredoxin reductase from human placenta is similar to the mechanisms of lipoamide dehydrogenase and glutathione reductase and is distinct from the mechanism of thioredoxin reductase from *Escherichia coli*. Proc. Natl. Acad. Sci. USA **94**:3621-3626.
9. **Arscott, L. D., C. Thorpe, and C. H. J. Williams.** 1981. Glutathione reductase from yeast. Differential reactivity of the nascent thiols in two-electron reduced enzyme and properties of a monoalkylated derivative. Biochemistry **20**:1513.
10. **Balch, W. E., and R. S. Wolfe.** 1978. Specificity and biological distribution of coenzyme M (2-mercaptoethanesulfonic acid). J. Bacteriol. **137**:256-263.
11. **Boyd, J. M., and S. A. E. A. Ellsworth.** 2006. Characterization of 2-bromoethanesulfonate as a selective inhibitor of the coenzyme M-dependent pathway and enzymes of aliphatic epoxide metabolism. J. Bacteriol. **188**:8062-8069.
12. **Boyd, J. M., D. D. Clark, M. A. Kofoed, and S. A. Ensign.** 2010. Mechanism of inhibition of aliphatic epoxide carboxylation by the coenzyme M analog 2-bromoethanesulfonate. J. Biol. Chem. **285**:25232-25242.
13. **Boyd, J. M., and S. A. Ensign.** 2005. Evidence for a metal-thiolate intermediate in alkyl group transfer from epoxypropane to coenzyme M and cooperative metal ion binding in epoxyalkane:CoM transferase. Biochemistry **44**:13151-13162.

14. **Clark, D. D., J. R. Allen, and S. A. Ensign.** 2000. Characterization of five catalytic activities associated with the NADPH:2-ketopropyl-coenzyme M [2-(2-ketopropylthio)ethanesulfonate] oxidoreductase/carboxylase of the *Xanthobacter* strain Py2 epoxide carboxylase. *Biochemistry* **39**:1294-1304.
15. **Clark, D. D., J. M. Boyd, and S. A. Ensign.** 2004. The stereoselectivity and catalytic properties of *Xanthobacter autotrophicus* 2-[(R)-2-hydroxypropylthio]ethanesulfonate dehydrogenase are controlled by interactions between C-terminal arginine residues and the sulfonate of coenzyme M. *Biochemistry* **43**:6763-6771.
16. **Clark, D. D., and S. A. Ensign.** 2002. Characterization of the 2-[(R)-2-hydroxypropylthio]ethanesulfonate dehydrogenase from *Xanthobacter* strain Py2: product inhibition, pH dependence of kinetic parameters, site-directed mutagenesis, rapid equilibrium inhibition, and chemical modification. *Biochemistry* **41**:2727-2740.
17. **Diekert, G., R. Jaenchen, and R. K. Thauer.** 1980. Biosynthetic evidence for a nickel tetrapyrrole structure of factor F430 from *Methanobacterium thermoautotrophicum*. *FEBS Lett.* **119**:118-120.
18. **Diekert, G., B. Klee, and R. K. Thauer.** 1980. Nickel, a component of factor F430 from *Methanobacterium thermoautotrophicum*. *Arch. Microbiol.* **124**:103-106.
19. **Ensign, S. A.** 2001. Microbial metabolism of aliphatic alkenes. *Biochemistry* **40**:5845-5853.

20. **Ermler, U., W. Grabarse, S. Shima, M. Goubeaud, and R. K. Thauer.** 1997. Crystal structure of methyl-coenzyme M reductase: the key enzyme of biological methane formation. *Science* **278**:1457-1462.
21. **Ghisla, S., and V. Massey.** 1989. Mechanisms of flavoprotein-catalyzed reactions. *Eur. J. Biochem.* **181**:1-17.
22. **Goenrich, M., F. Mahlert, E. C. Duin, C. Bauer, B. Jaun, and R. K. Thauer.** 2004. Probing the reactivity of Ni in the active site of methyl-coenzyme M reductase with substrate analogs. *J. Biol. Inorg. Chem.* **9**:691-705.
23. **Guengerich, F. P.** 1991. Reactions and significance of cytochrome P-450 enzymes. *J. Biol. Chem.* **266**:10019-10022.
24. **Gunsalus, R. P., J. A. Romesser, and R. S. Wolfe.** 1978. Preparation of coenzyme M analogues and their activity in the methyl coenzyme M reductase system of *Methanobacterium thermoautotrophicum*. *J. Bacteriol.* **17**:2374-2377.
25. **Hart, A., and M. W. Brown.** 1974. Propylene oxide as sterilizing agent. *Appl. Microbiol.* **28**:1069-1070.
26. **Hedderich, R., A. Berkessel, and R. K. Thauer.** 1990. Purification and properties of heterodisulfide reductase from *Methanobacterium thermoautotrophicum* (strain Marburg). *Eur. J. Biochem.* **193**:255-261.
27. **Jacobs, M. H. J., A. v. d. Wijngaard, M. Pentenga, and D. Janssen.** 1991. Characterization of the epoxide hydrolase from an epichlorohydrin-degrading *Pseudomonas* sp. *Eur. J. Biochem.* **202**:1217-1222.

28. **Jornvall, H., M. K. B. Persson, S. Atrian, R. Gonzalez-Duarte, J. Jeffery, and D. Ghosh.** 1995. Short-chain dehydrogenases/reductases (SDR). *Biochemistry* **34**:6003-6013.
29. **Karplus, P. A., and G. E. Schulz.** 1989. Substrate binding and catalysis by glutathione reductase as derived from refined enzyme: substrate crystal structure at 2 angstrom resolution. *J. Mol. Biol.* **210**:163-180.
30. **Krishnakumar, A. M., B. P. Nocek, D. D. Clark, S. A. Ensign, and J. W. Peters.** 2006. Structural basis for stereoselectivity in the (*R*)- and (*S*)-hydroxypropylthioethanesulfonate dehydrogenases. *Biochemistry* **45**:8831-8840.
31. **Krum, J. G., H. Ellsworth, R. R. Sargeant, G. Rich, and S. A. Ensign.** 2002. Kinetic and microcalorimetric analysis of substrate and cofactor interactions in epoxyalkane:CoM transferase, a zinc-dependent epoxidase. *Biochemistry* **41**:5005-5014.
32. **Krum, J. G., and S. A. Ensign.** 2000. Heterologous expression of bacterial epoxyalkane:coenzyme M transferase and inducible coenzyme M biosynthesis in *Xanthobacter* strain Py2 and *Rhodococcus rhodochrous* B276. *J. Bacteriol.* **182**:2629-2634.
33. **Kunz, R. C., M. Dey, and S. W. Ragsdale.** 2008. Characterization of the thioether product formed from the thiolytic cleavage of the alkyl-nickel bond in methyl-coenzyme M reductase. *Biochemistry* **47**:2661-2667.
34. **Kunz, R. C., Y. C. Horng, and S. W. Ragsdale.** 2006. Spectroscopic and kinetic studies of the reaction of bromopropanesulfonate with methyl-coenzyme M reductase. *J. Biol. Chem.* **281**:34663-34676.

35. **Mathews, R. G., and C. H. Williams Jr.** 1976. Measurement of the oxidation-reduction potentials for two-electron and four-electron reduction of lipoamide dehydrogenase from pig heart. *J. Biol. Chem.* **251**:3956-3964.
36. **McBride, B. C., and R. S. Wolfe.** 1971. A new coenzyme of methyl transfer, coenzyme M. *Biochemistry* **10**:2317-2324.
37. **Nakajima, K., T. Hashimoto, and Y. Yamada.** 1993. Two tropinone reductases with different stereospecificities are short-chain dehydrogenases evolved from a common ancestor. *Proc. Natl. Acad. Sci. USA* **90**:9591-9595.
38. **Nocek, B., S. E. Jang, M. S. Jeong, D. D. Clark, S. A. Ensign, and J. W. Peters.** 2002. Structural basis for CO₂ fixation by a novel member of the disulfide oxidoreductase family of enzymes, 2-ketopropyl-coenzyme M oxidoreductase/carboxylase. *Biochemistry* **41**:12907-12913.
39. **Pandey, A. S., D. W. Mulder, S. A. Ensign, and J. W. Peters.** 2011. Structural basis for carbon dioxide binding by 2-ketopropyl coenzyme M oxidoreductase/carboxylase. *FEBS Lett.* **585**:459-464.
40. **Pandey, A. S., B. Nocek, S. A. E. D. D. Clark, and J. W. Peters.** 2006. Mechanistic implications of the structure of the mixed-disulfide intermediate of the disulfide oxidoreductase, 2-ketopropyl-coenzyme M oxidoreductase/carboxylase. *Biochemistry* **45**:113-120.
41. **Rietveld, P., L. D. Arscott, A. Berry, N. S. Scrutton, M. P. Deonarain, R. N. Perham, and C. H. Williams Jr.** 1994. Reductive and oxidative half-reactions of glutathione reductase from *Escherichia coli*. *Biochemistry* **33**:13888-13895.

42. **S, H., J. P. Smits, M. J. v. d. Werf, F. Volkering, and J. A. M. deBont.** 1989. Metabolism of styrene oxide and 2-phenylethanol in the styrene-degrading *Xanthobacter* strain 124X. *Appl. Environ. Microbiol.* **55**:2800-2805.
43. **Salinas, A. E., and M. G. Wong.** 1999. Glutathione S-transferases--a review. *Curr. Med. Chem.* **6**:279-309.
44. **Schultz, P. G., K. G. Au, and C. T. Walsh.** 1985. Directed mutagenesis of the redox-active disulfide in the flavoenzyme mercuric ion reductase. *Biochemistry* **24**:6840-6848.
45. **Sliwa, D. A., A. M. Krishnakumar, J. W. Peters, and S. A. Ensign.** 2010. Molecular basis for enantioselectivity in the (*R*)- and (*S*)-hydroxypropylthioethanesulfonate dehydrogenases, a unique pair of stereoselective short-chain dehydrogenases/reductases involved in aliphatic epoxide carboxylation. *Biochemistry* **49**:3487-3498.
46. **Small, F. J., and S. A. Ensign.** 1997. Alkene monooxygenase from *Xanthobacter* strain Py2. *J. Biol. Chem.* **272**:24913-24920c
47. **Taylor, C. D., and R. S. Wolfe.** 1974. Structure and methylation of Coenzyme M (HSCH₂CH₂SO₃). *J. Biol. Chem.* **249**:4879-4885.
48. **Thauer, R. K.** 1998. Biochemistry of methanogenesis: a tribute to Marjory Stephenson. 1998 Marjory Stephenson Prize Lecture. *Microbiology* **144**:2377-2406.
49. **van Ginkel, C. G., and J. A. M. d. Bont.** 1986. Isolation and characterization of alkene-utilizing *Xanthobacter* spp. *Arch. Microbiol.* **145**:403-407.

50. **van Ginkel, C. G., H. G. J. Welten, and J. A. M. de Bont.** 1987. Oxidation of gaseous and volatile hydrocarbons by selected alkene-utilizing bacteria. *Appl. Environ. Microbiol.* **53**:2903-2907.
51. **Wade, D. R., S. C. Airy, and J. E. Sinsheimer.** 1978. Mutagenicity of aliphatic epoxides. *Mutat. Res.* **58**:217-223.
52. **Wallin, R., and T. M. Guenther.** 1997. Purification of warfarin-sensitive vitamin K epoxide reductase. *Methods Enzymol.*:395-407.
53. **Wallin, R., D. C. Sane, and S. M. Hutson.** 2002. Vitamin K 2, 3-epoxide reductase and the vitamin K-dependent [gamma]-carboxylation system. *Thromb. Res.* **108**:221-226.
54. **Wang, P. F., D. M. Veine, S. H. Ahn, and C. H. Williams Jr.** 1996. A stable mixed disulfide between thioredoxin reductase and its substrate, thioredoxin: preparation and characterization. *Biochemistry* **35**:4812-4819.
55. **Whitman, W. B., and R. S. Wolfe.** 1980. Presence of nickel in factor F430 from *Methanobacterium bryantii*. *Biochem. Biophys. Res. Commun.* **92**:1196-1201.
56. **Wolfe, R. S.** 1991. My kind of biology. *Annu. Rev. Biochem.* **45**:1-35.
57. **Zhou, Z. S., K. Peariso, J. Penner-Hahn, and R. Matthews.** 1999. Identification of the zinc ligands in cobalamin-independent methionine synthase (MetE) from *Escherichia coli*. *Biochemistry* **38**:15915-15926.

CHAPTER 2

MECHANISTIC CHARACTERIZATION OF 2-KPCC BY CHARACTERIZATION OF
H137A, H84A AND M140A SITE DIRECTED MUTANTS

ABSTRACT

In *Xanthobacter autotrophicus* strain Py2, epoxides are metabolized and converted to acetoacetate by a three step, four enzyme system. The final step in this pathway is catalyzed by NADPH:2-ketopropyl-CoM oxidoreductase/carboxylase (2-KPCC) and involves the reductive cleavage and carboxylation of 2-ketopropyl-CoM, yielding free CoM and acetoacetate. 2-KPCC is a member of the NAD(P)H:disulfide oxidoreductase (DSOR) family of enzymes, however 2-KPCC possesses several unique features that distinguish it from other members of this family, most notably the ability to cleave a thioether bond. As typical for DSOR enzymes, 2-KPCC contains two cysteine residues that are crucial for reductive catalysis. Atypical for DSOR enzymes, 2-KPCC contains a catalytic triad consisting of His84, His137 and a lone water molecule within the active site that is proposed to stabilize the enolacetone formed upon catalysis. Unique to DSOR members, but conserved in enzymes in the epoxide degradation pathway in *X. autotrophicus*, is the presence of a pair of methionine residues proposed to function in shielding the substrate molecule from electrostatic interactions. An expression vector was utilized to facilitate the expression, purification and characterization of H137A and H84A mutants, as well as M140A 2-KPCC. As expected, mutation of the distal histidine reduced redox dependent activity to 13-25% of the wild type enzyme, while mutation of the proximal histidine completely diminished enzymatic activity. 2-KPCC is also

capable of redox-independent activity, which was intriguingly not affected by mutation of either histidine residue. The M140A mutation in 2-KPCC resulted in an enzyme with a k_{cat} value 4 times lower than that of the wild type enzyme but with a K_m value 45 times higher, indicating a structural rather than catalytic role of the methionine residue.

INTRODUCTION

Xanthobacter autotrophicus strain Py2 is one of several bacteria that are capable of converting propylene to the more easily assimilated metabolite acetoacetate (12). Propylene is converted to *R*- and *S*-epoxypropane by insertion of oxygen across the olefin bond in a stereoselective manner (20). The metabolism of the epoxides to form acetoacetate is catalyzed by an inducible, three step, four enzyme system employing the unique cofactor Coenzyme M (CoM), which was originally believed to be restricted to methanogenic archaea (7, 15, 19, 23). The final step in this pathway is catalyzed by 2-ketopropyl-Coenzyme M [2-(2-Ketopropylthio)ethanesulfonate] oxidoreductase/carboxylase (2-KPCC), a member of the FAD-dependent NADPH:disulfide oxidoreductase (DSOR) family of enzymes and involves the reductive cleavage of 2-ketopropyl-CoM (2-KPC), yielding free CoM and the enolate of acetone (4, 10, 12, 21, 22). This product can then undergo carboxylation in the presence of CO₂ to form acetoacetate, or protonation in the absence of CO₂ to form acetone as shown in Figure 2-1 (10). In addition to the two aforementioned catalytic activities, 2-KPCC has been shown to catalyze three other reactions which are [1] the NADP⁺-dependent synthesis of 2-KPC from acetoacetate and CoM; [2] acetoacetate decarboxylation to form acetone and CO₂;

and [3] acetoacetate/ $^{14}\text{C}\text{O}_2$ exchange to form $^{14}\text{C}_1$ -acetoacetate and CO_2 , with reactions [2] and [3] being redox-independent (10).

While typical DSOR members, like glutathione reductase and thioredoxin reductase cleave a disulfide bond (5, 6), 2-KPCC is distinctive in that it is the only

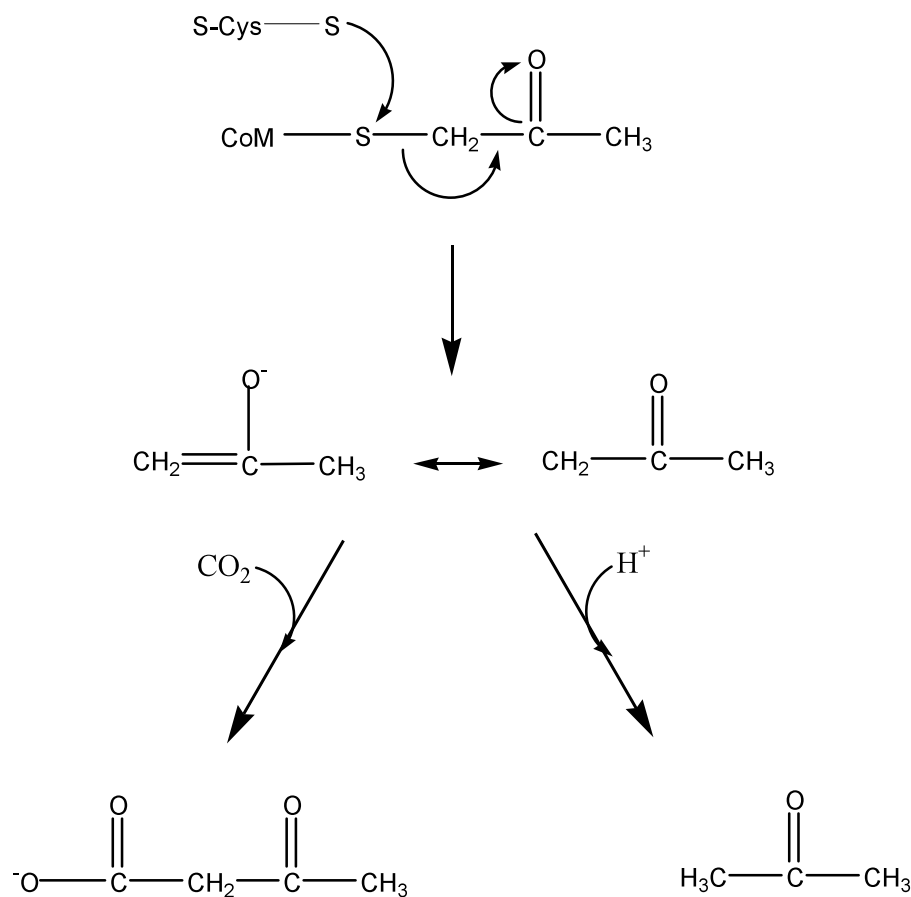


Figure 2-1. Schematic representation illustrating the fate of the enolate intermediate formed upon attack of the CoM thiol by Cys82 of 2-KPCC, which can undergo carboxylation, or in the absence of CO_2 , protonation.

identified member of the DSOR family that is also a carboxylase, and in addition, employs a novel approach to carboxylation in that it is the only carboxylase known to form a carbanionic nucleophile from reductive cleavage of a thioether substrate without the requirement of thiamin pyrophosphate (TPP) (2, 10).

Although 2-KPCC is capable of both protonating and carboxylating the enolate intermediate formed during catalysis, carboxylation is favored to the extent that in the presence of CO₂, no detectable acetone is formed. Preferential carboxylation is thought to be mediated in part by the stabilization of the enolacetone intermediate formed. Previous mechanistic studies indicated enolate stabilization by either [1] catalytic acid mediated proton donation to the carbonyl oxygen or [2] electrostatic stabilization using a positively charged amino acid side chain(s) (10). Elucidation of the crystal structure of 2-KPCC indicates an ordered water molecule within hydrogen bonding distance of the keto group of the substrate (16). Two histidine residues orient this water molecule within the active site, and acting together as a catalytic triad, allow the water molecule to serve as a proton donor involved in stabilizing the enolacetone intermediate and facilitating the reductive cleavage of the thioether linkage (Figure 2-2) (16).

Conserved between the enzymes in the last two steps in the epoxide degradation pathway, are two methionine residues believed to play a role in shielding the substrate from nonproductive electrostatic interactions (13, 16). Mutation of these residues in *R*-HPCDH revealed enzymes with a slightly lower k_{cat} values, but much lower K_m values than the wild type enzyme (Sliwa, unpublished). It is hypothesized that mutation of these methionine residues, Met140 and Met361 in 2-KPCC would generate an enzyme that exhibited similar changes in kinetic parameters.

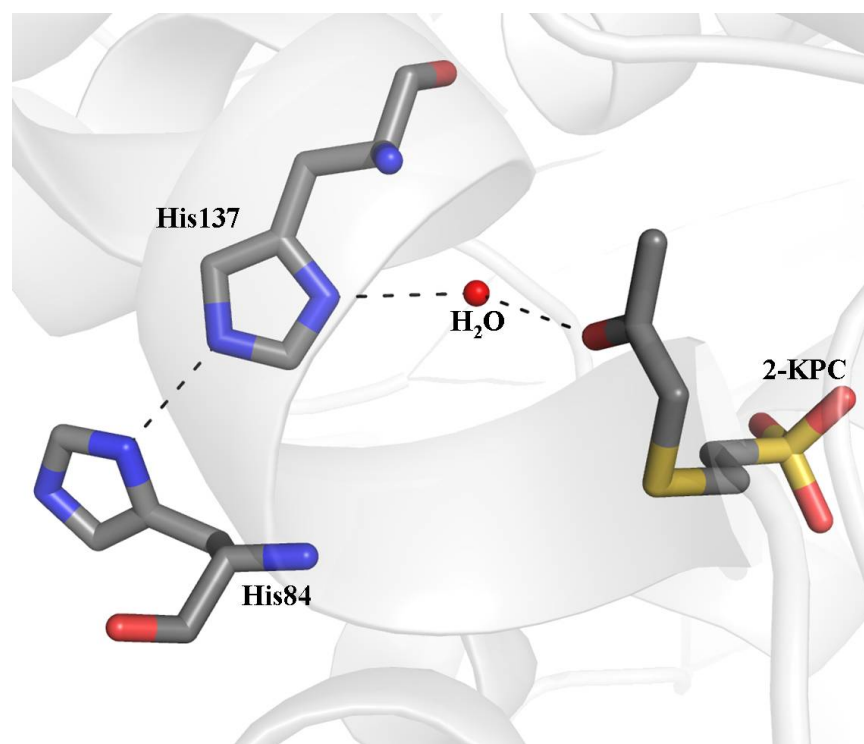


Figure 2-2. Active site of 2-KPCC with the substrate, 2-KPC bound. His137 coordinates an ordered water molecule in the active site and is indirectly coordinated by His84, forming a purported catalytic triad involved in stabilizing the enolate intermediate formed during catalysis.

In these studies, a recombinant expression system was utilized to express high levels of soluble, active 2-KPCC and to allow the generation of desired variants. The catalytic activities of 2-KPCC have been examined upon alteration of the two histidine residues comprising the catalytic triad to alanine residues, His137, involved in directly coordinating the water molecule, termed the proximal histidine, and His84 which coordinates His137, termed the distal histidine, as well as alteration of Met140 to alanine. Although generation of M361A 2-KPCC was unsuccessful, mutation of one of the

conserved methionine residues was still able to provide considerable insight into the roles of these methionine residues in 2-KPCC.

As expected, mutation of the proximal histidine residue completely diminished the activity of 2-KPCC, while H84A 2-KPCC exhibited 23-25% of wild type 2-KPCC activity, with regard to the physiologically relevant reactions. The M140A 2-KPCC exhibited a k_{cat} value 25% of wild type 2-KPCC but with a K_m 45 times higher than for that of the wild type enzyme. This work contributes to the greater understanding of the versatility of the DSOR family of enzymes.

METHODS

Materials. Commercially available compounds used were of analytical grade and purchased from either Sigma-Aldrich Chemicals or Fisher Scientific. 2-(2-Keto-propylthio)ethanesulfonate (2-KPC) was synthesized as described previously (1). All oligonucleotides were purchased from Integrated DNA Technologies.

Site Directed Mutagenesis. Site directed mutagenesis of pDW1 was carried out utilizing the Quikchange[®] Site Directed Mutagenesis Kit (Stratagene) according to the manufacturer's protocols. The sequences of the primer pairs used to create the desired mutations are as follows: H137A, 5'-GAA GTT CAT GAT GCC GGC CGG GCC GTT GCG CC-3' and CGC AAC GGC CCG GCC GGC ATCATG AAC TTC CA-3'; H84A, 5'-CAC GCA CGC ATT GGC CGG GCA CGA GCC GCC-3' and 5'-CCG CCG AGC ACG GGC CGG TTA CGC ACG CAC-3'; M140A, 5'-CGG CCC GCA CGG CAT CGC GAA CTT CCA GTC CAA GG-3' and 5'-CCT TGG ACT GGA AGT TCG CGA

TGC CGT GCG GGC CG-3'. Mutations were confirmed by primer extension sequencing at SeqWright DNA Technology Services (Houston, TX).

Growth Media. *E. coli* Top10 cells were grown in Luria-Bertani Rich (LB-Rich) broth containing ampicillin (100 µg/mL). The LB-Rich media contained the following components per liter: 20 g of tryptone, 15 g of yeast extract, 2 g of K₂HPO₄, 1 g of KH₂PO₄, and 8 g of NaCl.

Growth of Bacteria. All bacteria were grown at 37°C. *E. coli* Top10 cells that had been transformed with the pDW1 or corresponding mutant plasmid were plated and grown overnight. A single colony from this plate was used to grow a 25 mL liquid culture to an A₆₀₀ of 0.6 for preparation of 25% glycerol (v/v) stocks that were stored at -80°C until use. For use, cells from a frozen stock were inoculated into 125 mL of LB-Rich media and grown to an A₆₀₀ between 0.6 and 1.0. This culture was used as the inoculum for a 15 L capacity microferm fermentor (New Brunswick Scientific) containing 12 L of LB-Rich media supplemented with riboflavin (15 mg/L) and antifoam A (0.005% v/v). Cells were allowed to grow at 37°C with stirring at 400 rpm and forced aeration to an OD₆₀₀ between 0.6 and 1.0. At this time, the temperature was reduced to 30°C, arabinose was added to 0.02% and the cells were allowed to grow at this temperature for 6 h. Cells were concentrated using a tangential flow filtration system (Millipore) and pelleted by centrifugation. Cell paste was drop frozen in liquid nitrogen and stored at -80°C.

Purification of Recombinant 2-KPCC. Cell paste was resuspended in 3 volumes of buffer A (50 mM Tris, 1 mM DTT, 0.1 mM EDTA, 5% glycerol v/v) with DNase I (0.03 mg/mL) and lysozyme (0.03 mg/mL) and thawed at 30°C with shaking. All

subsequent treatments were performed either on ice or at 4°C. Cell suspension was passed three times through a French pressure cell (16000 psi) and clarified by centrifugation (184000 RCF). Clarified cell extract was applied to a 0.5 x 5.0 cm column of Ni-NTA Superflow (Pharmacia Biotech) at 7.0 mL/min. The column was then washed with 4 column volumes of buffer A and the bound sample was eluted with a 15 column volume gradient from 0-400 mM imidazole, although most protein eluted during the wash phase. The purification was followed using SDS-PAGE analysis. Appropriate fractions were pooled and, the solution was incubated at 4°C with gentle stirring while (NH₄)₂SO₄ was added to 800 mM, and then applied to a 2.6 x 5.5 cm column of phenyl sepharose that had been equilibrated with buffer C (buffer A + 800 mM (NH₄)₂SO₄). The column was then washed with 4 column volumes buffer C and bound protein was eluted with a 15 column volume gradient from 0-100% buffer A followed by an additional five column volumes buffer A. Appropriate fractions were pooled and concentrated by ultrafiltration using a YM30 membrane (Amicon) and frozen dropwise in liquid nitrogen for storage at -80°C.

Protein Concentration Determination. 2-KPCC concentrations were determined by using the previously determined extinction coefficient (ϵ_{450} of 11828 M⁻¹•cm⁻¹) (3).

SDS-PAGE and Immunoblotting Procedures. SDS-PAGE (12% T) was performed following the Laemmli procedure (14). Electrophoresed proteins were visualized by staining with Coomassie blue. The apparent molecular masses of polypeptides were determined by comparison with R_f values of standard proteins.

Coupled Spectrophotometric Assay for 2-KPCC Carboxylation Activity. A continuous spectrophotometric assay was utilized that couples acetoacetate production by 2-KPCC to acetoacetate reduction and concomitant NADH oxidation by β -Hydroxybutyrate Dehydrogenase (β -HBDH) (8). Purification of β -HBDH for use in the assay was performed as described previously (9). Assays were conducted in 2 mL anaerobic quartz cuvettes that contained a total reaction volume of 1 mL. Assays contained 0.125 mg 2-KPCC, 0.345 mg β -HBDH, 10 mM DTT, 0.2 mM NADH and 60 mM carbonate species (added as 33.5 mM CO₂ gas plus 26.5 mM KHCO₃) in 100 mM Tris buffer, pH 7.4. Reactions were allowed to equilibrate to 30°C and assays were initiated by the addition of 2.5 μ mol 2-KPC. Acetoacetate production by 2-KPCC and subsequent reduction by NADH was quantified by monitoring the decrease in absorbance (A_{340}) associated with the oxidation of NADH in a Shimadzu UV160U spectrophotometer containing a water-jacketed cell holder for temperature control.

2-Ketopropyl-CoM Protonation Assays. Assays were performed as described previously (10). Assays were conducted in 9 mL sealed serum vials with a total reaction volume of 1 mL. Each assay contained 0.125 mg 2-KPCC and 10 mM DTT in 100 mM Tris buffer, pH 7.4. Assay vials were incubated in a 30°C shaking water bath and assays were initiated by the addition of 2.5 μ mol 2-KPC. Acetone formation was quantified as a function of time using gas chromatography as described previously (11).

Acetoacetate Decarboxylation Assay. Assays were performed as described previously (10). Assays were conducted in 9 mL sealed serum vials with a total reaction volume of 1 mL. Vials were depleted of carbonate species by including a KOH-containing trap as described previously (11). Each assay contained 250 mM acetoacetate

and 5 mM CoM in 100 mM Tris buffer, pH 7.4. Assay vials were incubated in a 30°C shaking water bath and assays were initiated by addition of 0.125 mg 2-KPCC. Acetone was quantified by gas chromatography as described previously (11). Background rates of spontaneous acetoacetate decarboxylation were subtracted from all assays.

Continuous Spectrophotometric Assay for 2-Ketopropyl-CoM Formation.

Assays were performed as described previously (10). Assays were conducted in 2 mL anaerobic quartz cuvettes with a total reaction volume of 1 mL. Each assay contained 0.125 mg 2-KPCC, 5 mM NADP⁺, 5 mM CoM, and 100 mM acetoacetate in 100 mM Tris buffer, pH 7.4. Reactions were allowed to equilibrate to 30°C and assays were initiated by the addition of acetoacetate. Formation of 2-KPC was quantified by monitoring the increase in absorbance (A_{340}) associated with the production of NADPH in a Shimadzu UV160U spectrophotometer containing a water-jacketed cell holder for temperature control.

Data Analysis. Kinetic constants (K_m and V_{max}) were calculated by fitting initial rate data to the Michaelis-Menten equation using the software SIGMAPLOT.

RESULTS

Redox-dependent Reactions of H84A and H137A 2-KPCC. The two histidine mutants created were kinetically characterized relative to the recombinant wild type enzyme with respect to the redox-dependent reactions of 2-KPCC, protonation of the enolacetone intermediate formed to form acetone, carboxylation of the enolacetone intermediate formed to form acetoacetate and the reverse of the physiological reaction, formation of 2-KPC from acetoacetate and CoM. His137 is directly involved in

coordinating the lone water molecule in the active site of 2-KPCC and as expected, when modified to alanine, the enzyme had minimal to no activity in any of the three redox-dependent reactions studied (Table 2-1).

Table 2-1. Redox-dependent activities of 2-KPCC mutants.

	Protonation	Carboxylation	Formation of 2-KPC
wt 2-KPCC	79 ± 14 mU	278 ± 47 mU	48 ± 2 mU
H84A 2-KPCC	18 ± 1 mU	37 ± 4.2 mU	12 ± 0.57 mU
H137A 2-KPCC	nd	18 ± 1 mU	1 ± 0.1 mU

*One unit of activity (U) is defined as 1 μmol of product formed per minute per mg of protein.

For the H137A 2-KPCC mutant, no protonation activity was detected while the enzyme retained only 6% of wild type carboxylation activity, and 2% of the wild type rate of the formation of 2-KPC. His84 is indirectly involved in coordinating the lone water molecule in the active site through His137, and when modified to alanine, the activity of 2-KPCC is significantly decreased. The H84A 2-KPCC mutant exhibited activities of 23%, 13% and 25% of the wild type enzyme activity with regard to the protonation, carboxylation, and formation of 2-KPC activities of 2-KPCC respectively. The results of these studies demonstrate that both histidine residues of the purported catalytic triad are essential for efficient catalysis. This evidence lends further support to the hypothesis that these two histidine residues are directly involved in stabilization of the enolate intermediate through an ordered water molecule within the active site.

Redox-independent Reactions of H84A and H137A 2-KPCC. Although acetoacetate decarboxylates spontaneously, 2-KPCC has been shown to accelerate the rate of acetoacetate decarboxylation in the presence of CoM. Unlike the physiologically relevant reactions of 2-KPCC, which require NADP⁺/NADPH, acetoacetate

decarboxylation is independent of a redox active cofactor. While the mechanism of 2-KPCC catalyzed acetoacetate decarboxylation is presumably through an enolacetone intermediate, mutation of either the proximal or distal histidine residue resulted in an enzyme that was more active than the wild type enzyme (Figure 2-3). This is a result that was also observed for mutation of each of two active site cysteine residues. One possible explanation for this observation is that mutation of a larger residue, such as cysteine or histidine, to a much smaller alanine, creates a larger active site allowing easier access to acetoacetate molecules.

Substrate access to the active site of 2-KPCC is by a narrow channel and is unlike that of conventional DSOR enzymes. The elucidation of the crystal structure has shown that 2-KPCC undergoes a conformational shift upon substrate binding, closing the channel and presumably limiting solvent access to the active site to prevent protonation of the enolacetone formed (16). Because 2-KPCC catalyzed acetoacetate decarboxylation is not observed in the absence of CoM, it is thought that perhaps orientation of CoM in the active site induces a conformational change, which allows for the channel closing and more efficient catalysis. Compounds such as ethanethiol, ethanesulfonate, and taurine have been studied for their ability to substitute for CoM in acetoacetate decarboxylation catalysis, but none of the compounds were able to stimulate activity above that of protein alone (data not shown).

Although His137 is directly involved in ordering a water molecule within the active site to serve as a proton donor for stabilization of the enolate intermediate formed during catalysis, the crystal structure of 2-KPCC with the interchange thiol-CoM mixed disulfide trapped shows the absence of the histidine ordered water molecule and the side

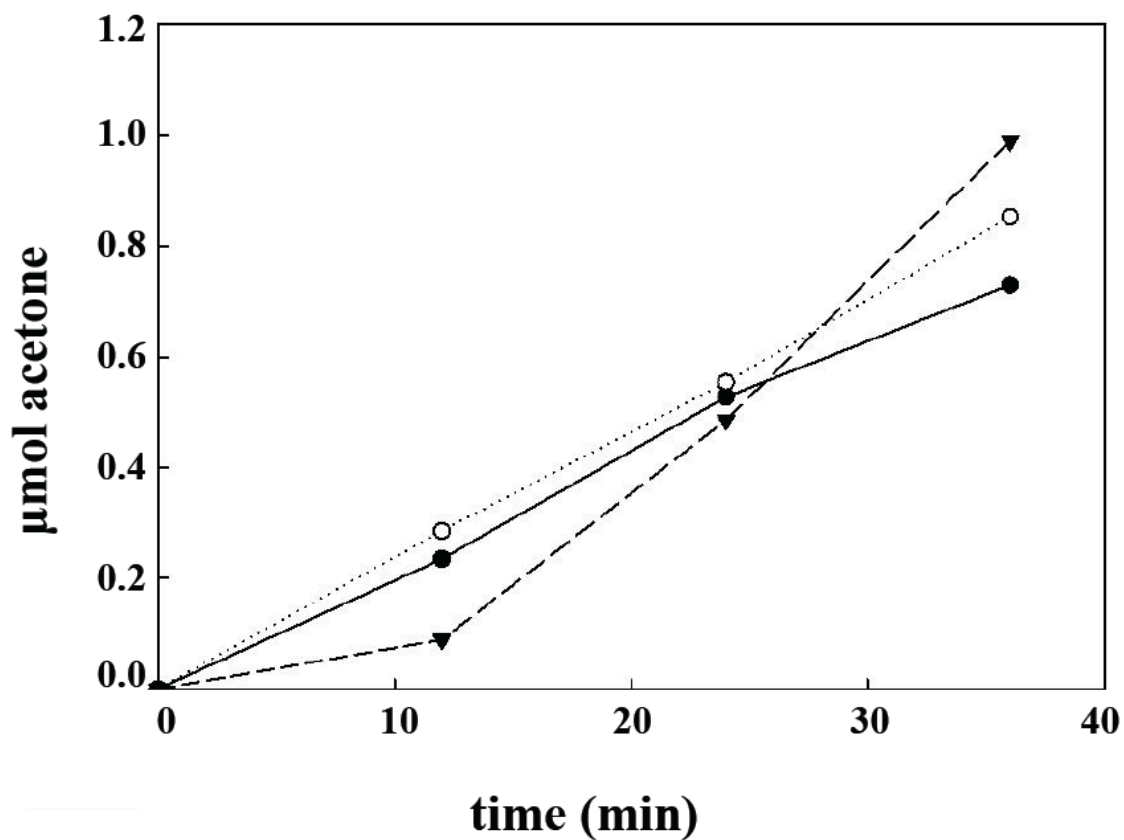


Figure 2-3. Time course of acetone production as a product of 2-KPCC catalyzed acetoacetate decarboxylation. Assays were performed in duplicate and contained the standard assay mixture as described in Methods. Assays contained 0.125 mg 2-KPCC: ●, wt 2-KPCC; ○, H84A 2-KPCC; ▼ H137A 2-KPCC.

chain of His137 rotated 180° away from the active site cavity (18). This structure may be similar to the conformation of 2-KPCC with CoM bound and is in agreement with the observation that the neither His84 nor His137, and hence, enolate stabilization, is important for the rate enhancement of acetoacetate decarboxylation.

The most recent crystal structure of 2-KPCC solved (17), shows CO₂ bound at the bottom of a hydrophobic channel at the hydrophobic interface between the two subunits

of 2-KPCC. Perhaps the stabilization of released CO₂ from the decarboxylation of acetoacetate also lends to the catalytic rate enhancement of acetoacetate decarboxylation by 2-KPCC.

Analysis of M140A 2-KPCC. There are many striking similarities between the active site of 2-KPCC and the active sites of the dehydrogenases catalyzing the penultimate step in the epoxide degradation pathway. Included are two signature positively charged residues, two arginines or an arginine and lysine, which function to coordinate the negatively charged sulfonate group of CoM, and a bulky residue, either phenylalanine or tryptophan, which functions in the active site as a backstop, preventing the translocation of the substrate. Perhaps more interesting is the conserved presence of two methionine residues, Met187 and Met192 in *R*-hydroxypropyl-CoM dehydrogenase (*R*-HPCDH) and Met140 and Met361 in 2-KPCC (Figure 2-4). It is presumed that these methionine residues function to shield the substrate sulfonate group from electrostatic interactions with the surrounding environment. Previous analysis of methionine to alanine mutations in *R*-HPCDH revealed an enzyme with k_{cat} values 2-4 times lower than that of wild type *R*-HPCDH and K_m values 18-24 times lower than that of the wild type enzyme.

Ideally both methionine to alanine mutations (M140A, M361A) would have been made in 2-KPCC, however the many attempts at creating the M361A mutant were unsuccessful. Nonetheless, the generation and characterization of M140A still provides relevant insights into the role of these methionine residues in the active site of 2-KPCC. The M140A enzyme exhibited saturation kinetics with regard to the substrate 2-KPC and afforded an apparent $K_m = 6.37 \pm 0.82$ mM and $V_{max} = 75.6 \pm 3.3$ mU/mg (Figure 2-5).

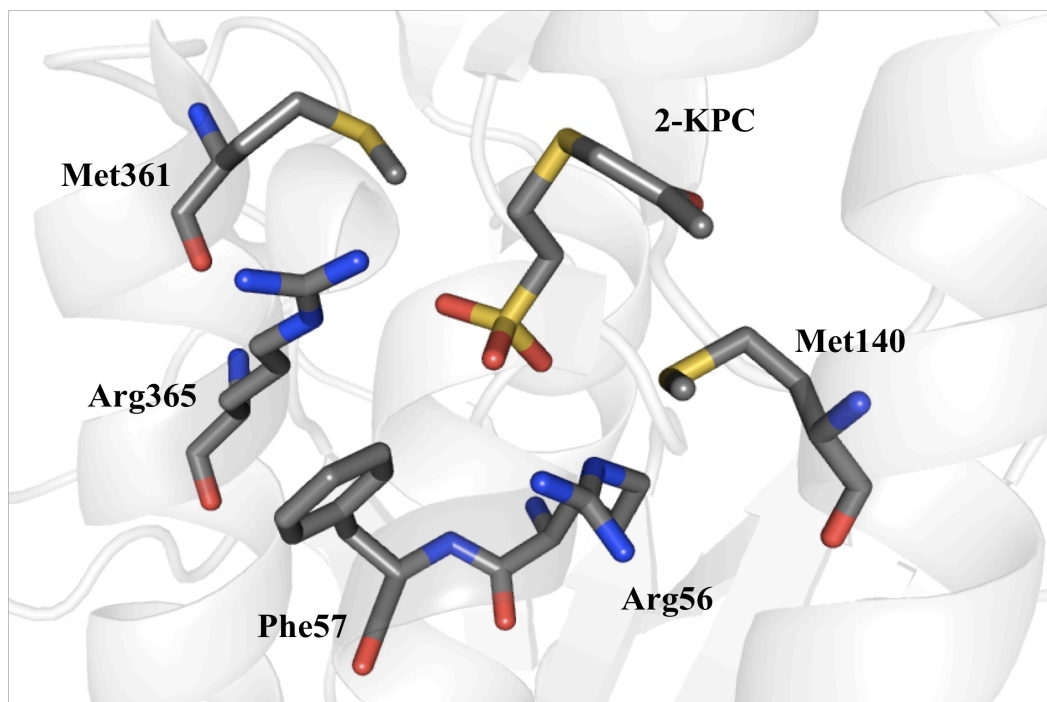


Figure 2-4. Active site of 2-KPCC showing the position of 2-KPC where the sulfonate is oriented by Arg56 and Arg365. Phe57 serves as a backstop preventing translocation of the substrate while the two flanking methionine residues, Met361 and Met140 presumably shield the negatively charged sulfonate group and positively charged arginine residues from nonproductive electrostatic interactions.

Kinetic characterization of the M140A 2-KPCC mutant revealed an enzyme with a k_{cat} only 3 times lower than the wild type enzyme, but with a K_m close to 45 fold higher (Table 2-2). These results are nearly identical to those obtained with *R*-HPCDH.

Additionally, the methionine residues have also been shown to function in aiding in the stereospecificity of *R*- and *S*-HPCDH, in contrast to 2-KPCC where both the reactant and product are achiral.

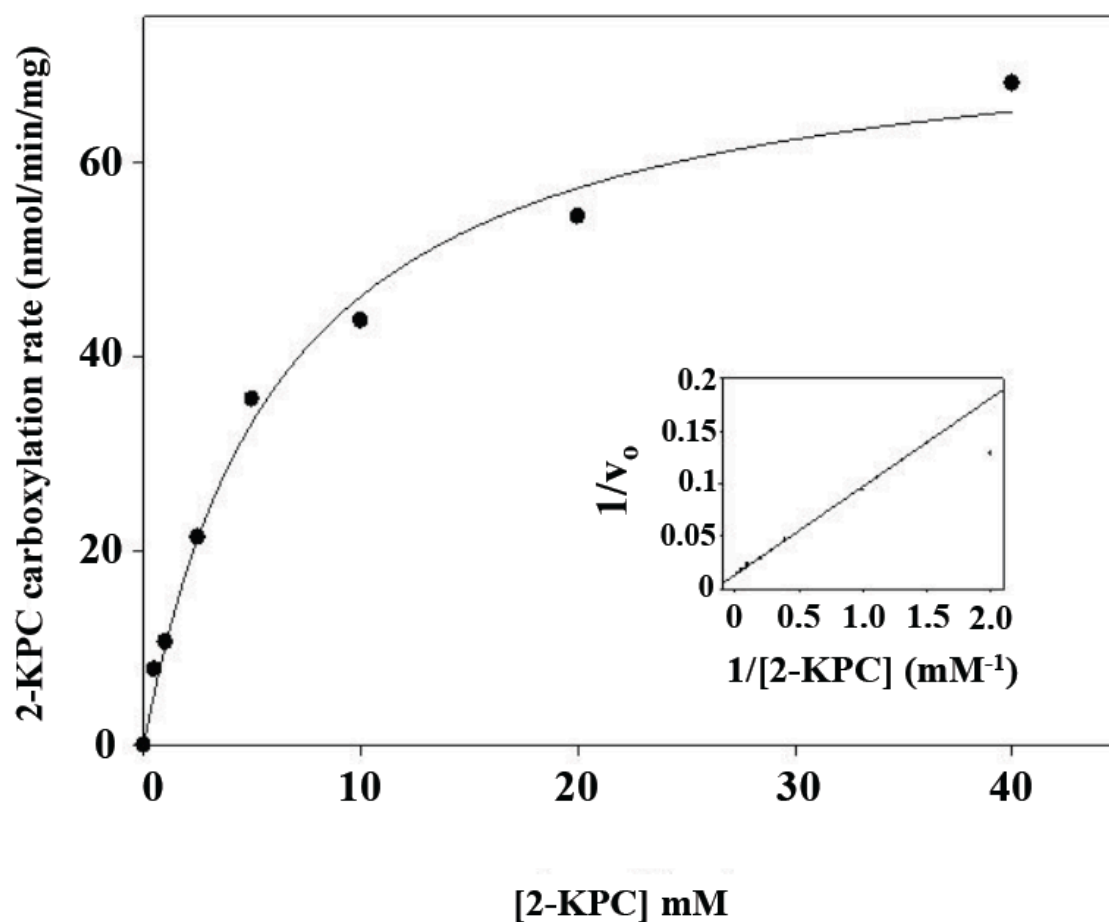


Figure 2-5. Initial velocities of 2-KPC cleavage and carboxylation to form acetoacetate as a function of [2-KPC]. Assays were performed in duplicate and contained the standard assay mixture as described in Methods with 0.125 mg 2-KPCC and 0-40 mM 2-KPC. Data points were fit to a rectangular hyperbola as described by the standard form of the Michaelis-Menten equation. Inset, nonlinear regression from fit of experimental data to Michaelis-Menten equation.

Table 2-2. Comparison of kinetic parameters between wild type and M140A 2-KPCC.

	K_m (mM)	Change in K_m (x-fold)	k_{cat} (min ⁻¹)	Change in k_{cat} (x-fold)	k_{cat}/K_m
wild-type	0.142 ± 0.02	1	11.6	1	83.1
M140A	6.37 ± 0.82	45	4.3	3	0.74

DISCUSSION

This chapter highlights two of the features that set 2-KPCC apart from other members of the DSOR family. The initial mechanism proposed for 2-KPCC indicated the formation of an enolate intermediate during catalysis (10). While the crystal structure data for 2-KPCC supported this mechanism and indicated enolate stabilization by the presence of a water molecule ordered directly and indirectly by two histidine residues, kinetic studies of 2-KPCC mutants had yet to confirm this observation. Mutation of His137, the proximal histidine, prevented ordering of the water molecule in the active site and was determined to be essential for catalysis. When only the distal histidine, His84, was mutated, the enzyme was still capable of catalyzing all redox-dependent reactions, albeit, at a rate of only approximately 25% of that of the wild type enzyme. These observations further emphasize the important roles that these two histidines play in the physiologically relevant reactions catalyzed by 2-KPCC.

With regard to acetoacetate decarboxylation, it was surprising to find that both of the histidine mutants had activities comparable to, and even slightly higher than the wild type enzyme. It had been previously assumed that the enzyme catalyzed acetoacetate decarboxylation proceeded through an enolate intermediate presumably stabilized by the oriented water molecule in the active site. Further analysis of the 2-KPCC structure solved with the mixed disulfide intermediate formed has indicated, in addition to the rotation of the His137 side chain and absence of the ordered water molecule, an alternate anion binding pocket similar to that created by the two arginine residues responsible for orienting the CoM sulfonate of 2-KPC (18). It is hypothesized that this binding pocket, composed of Gln509 and His506, stabilizes the negatively charged carboxylate moiety

during the formation of acetoacetate. As 2-KPCC catalyzed acetoacetate decarboxylation, is CoM-dependent, perhaps the binding of CoM in the active site enhances productive acetoacetate orientation to the alternate anion binding site, allowing for more efficient catalysis.

Also unique to DSOR enzymes, is the highly hydrophobic active site of 2-KPCC, which is believed to play a pertinent role in isolating the active site from unrestricted solvent access, thereby promoting the more metabolically favorable production of acetoacetate as opposed to acetone that would be produced by unlimited access of protons to the active site. Included in the hydrophobic architecture of the 2-KPCC active site, are two methionine residues, which are also interestingly conserved in both *R*- and *S*-HPCDH, which catalyze the formation of 2-KPC just subsequent to it being cleaved and carboxylated by 2-KPCC. While methionine residues have been shown to play many roles in enzyme active sites, the studies of M140A in this chapter, complemented by studies of methionine mutants in *R*- and *S*-HPCDH, fulfill the objective of shielding the negatively charged sulfonate group of 2-KPC and the positively charged coordinating arginine residues from unproductive electrostatic interactions. The similar active site architectures of 2-KPCC and *R*- and *S*-HPCDH also call into question whether or not the conserved residues may serve as a sort of “signature” for as yet unidentified enzymes which utilize CoM bound substrates.

REFERENCES

1. **Allen, J. R., D. D. Clark, J. G. Krum, and S. A. Ensign.** 1999. A role for coenzyme M (2-mercaptoethanesulfonic acid) in a bacterial pathway of aliphatic epoxide carboxylation. *Proc. Natl. Acad. Sci. USA* **96**:8432-8437.
2. **Allen, J. R., and S. A. Ensign.** 1996. Carboxylation of epoxides to β -keto acids in cell extracts of *Xanthobacter* strain Py2. *J. Bacteriol.* **178**:1469-1472.
3. **Allen, J. R., and S. A. Ensign.** 1997. Characterization of three protein components required for functional reconstitution of the epoxide carboxylase multienzyme complex from *Xanthobacter* strain Py2. *J. Bacteriol.* **179**:3110-3115.
4. **Allen, J. R., and S. A. Ensign.** 1997. Purification to homogeneity and reconstitution of the individual components of the epoxide carboxylase multiprotein enzyme complex from *Xanthobacter* strain Py2. *J. Biol. Chem.* **272**:32121-32128.
5. **Arscott, L. D., S. Gromer, R. H. Schirmer, K. Becker, and C. H. Williams Jr.** 1997. The mechanism of thioredoxin reductase from human placenta is similar to the mechanisms of lipoamide dehydrogenase and glutathione reductase and is distinct from the mechanism of thioredoxin reductase from *Escherichia coli*. *Proc. Natl. Acad. Sci. USA* **94**:3621-3626.
6. **Arscott, L. D., C. Thorpe, and C. H. J. Williams.** 1981. Glutathione reductase from yeast. Differential reactivity of the nascent thiols in two-electron reduced enzyme and properties of a monoalkylated derivative. *Biochemistry* **20**:1513.

7. **Balch, W. E., and R. S. Wolfe.** 1978. Specificity and biological distribution of coenzyme M (2-mercaptoethanesulfonic acid). *J. Bacteriol.* **137**:256-263.
8. **Boyd, J. M., D. D. Clark, M. A. Kofoed, and S. A. Ensign.** 2010. Mechanism of inhibition of aliphatic epoxide carboxylation by the coenzyme M analog 2-bromoethanesulfonate. *J. Biol. Chem.* **285**:25232-25242.
9. **Boyd, J. M., and S. A. Ensign.** 2005. ATP-dependent enolization of acetone by acetone carboxylase from *Rhodobacter capsulatus*. *Biochemistry* **44**:8543-8553.
10. **Clark, D. D., J. R. Allen, and S. A. Ensign.** 2000. Characterization of five catalytic activities associated with the NADPH:2-ketopropyl-coenzyme M [2-(2-ketopropylthio)ethanesulfonate] oxidoreductase/carboxylase of the *Xanthobacter* strain Py2 epoxide carboxylase. *Biochemistry* **39**:1294-1304.
11. **Clark, D. D., and S. A. Ensign.** 1999. Evidence for an inducible nucleotide-dependent acetone carboxylase in *Rhodococcus rhodochrous* B276. *J. Bacteriol.* **181**:2752-2758.
12. **Ensign, S. A., and J. R. Allen.** 2003. Aliphatic epoxide carboxylation. *Annu. Rev. Biochem.* **72**:55-76.
13. **Krishnakumar, A. M., B. P. Nocek, D. D. Clark, S. A. Ensign, and J. W. Peters.** 2006. Structural basis for stereoselectivity in the (*R*)- and (*S*)-hydroxypropylthioethanesulfonate dehydrogenases. *Biochemistry* **45**:8831-8840.
14. **Laemmli, U. K.** 1970. Cleavage of structural proteins during the assembly of the head of bacteriophage T4. *Nature* **227**:680-685.
15. **McBride, B. C., and R. S. Wolfe.** 1971. A new coenzyme of methyl transfer, coenzyme M. *Biochemistry* **10**:2317-2324.

16. **Nocek, B., S. E. Jang, M. S. Jeong, D. D. Clark, S. A. Ensign, and J. W. Peters.** 2002. Structural basis for CO₂ fixation by a novel member of the disulfide oxidoreductase family of enzymes, 2-ketopropyl-coenzyme M oxidoreductase/carboxylase. *Biochemistry* **41**:12907-12913.
17. **Pandey, A. S., D. W. Mulder, S. A. Ensign, and J. W. Peters.** 2011. Structural basis for carbon dioxide binding by 2-ketopropyl coenzyme M oxidoreductase/carboxylase. *FEBS Lett.* **585**:459-464.
18. **Pandey, A. S., B. Nocek, S. A. E. D. D. Clark, and J. W. Peters.** 2006. Mechanistic implications of the structure of the mixed-disulfide intermediate of the disulfide oxidoreductase, 2-ketopropyl-coenzyme M oxidoreductase/carboxylase. *Biochemistry* **45**:113-120.
19. **Thauer, R. K.** 1998. Biochemistry of methanogenesis: a tribute to Marjory Stephenson. 1998 Marjory Stephenson Prize Lecture. *Microbiology* **144**:2377-2406.
20. **van Ginkel, C. G., and J. A. M. de Bont.** 1986. Isolation and characterization of alkene-utilizing *Xanthobacter* spp. *Arch. Microbiol.* **145**:403-407.
21. **Weijers, C. A. G. M., J. Jongejan, M. C. R. Franssen, A. de Groot, and J. A. M. de Bont.** 1995. Dithiol- and NAD-dependent degradation of epoxyalkanes by *Xanthobacter* Py2. *Appl. Microbiol. Biotechnol.* **42**:775-781.
22. **Westphal, A. H., J. Swaving, L. Jacobs, and A. de Kok.** 1998. Purification and characterization of a flavoprotein involved in the degradation of epoxyalkanes by *Xanthobacter* Py2. *Eur. J. Biochem.* **257**:160-168.
23. **Wolfe, R. S.** 1991. My kind of biology. *Annu. Rev. Biochem.* **45**:1-35.

CHAPTER 3

COMPLETED STUDIES OF C87A and C82A 2-KPCC AND COMPARATIVE SPECTRAL ANALYSIS OF C82A AND 2-BROMOETHANESULFONATE MODIFIED 2-KPCC¹

ABSTRACT

Characteristic and essential to all members of the disulfide oxidoreductase (DSOR) family of enzymes is the presence of a redox active disulfide pair that facilitate electron movement from a bound flavin to the substrate. Previous studies have indicated that mutation of either of these residues in 2-KPCC renders the enzyme inactive with regard to redox dependent reactions, however both the C82A and C87A 2-KPCC mutants catalyze redox independent acetoacetate decarboxylation at rates 204% and 181%, respectively, of the wild type enzyme. While DSOR enzymes typically catalyze the reductive cleavage and protonation of a substrate disulfide bond, 2-KPCC, a novel member of this family, catalyzes reductive cleavage of a thioether bond and subsequent carboxylation of the intermediate formed. Necessary to promote carboxylation over protonation of the substrate, and in stark contrast to other DSOR enzymes, 2-KPCC has a highly hydrophobic active site. Contributing to this architecture is the presence of a phenylalanine residue (Phe501) in place of a highly conserved histidine residue in other members of this family. The replacement of histidine with a hydrophobic phenylalanine in close proximity to the redox active cysteine pair has been shown to greatly increase the

¹Figure 3-3 was originally published in the Journal of Biological Chemistry. 2010. Boyd, JM; Clark, DD; Kofoed, MA; Ensign, SA. 285:25232-25242 © the American Society for Biochemistry and Molecular Biology.

pK_a of the flavin thiol, Cys87, relative to other DSOR enzymes. In this chapter, two methods were used to determine the pK_a of the flavin thiol of 2-KPCC to be approximately 8.75, including site-directed mutagenesis, and modification of the proximal thiol, Cys82, by the inhibitor and alkylating agent 2-bromoethanesulfonate.

INTRODUCTION

The final step in epoxide metabolism in *Xanthobacter autotrophicus* strain Py2 is catalyzed by the atypical member of the disulfide oxidoreductase (DSOR) family, NADPH:2-ketopropyl-Coenzyme M oxidoreductase/carboxylase (2-KPCC). Characteristic of DSOR enzymes, 2-KPCC contains a flavin cofactor and two conserved cysteine residues essential for reductive catalysis (10). Termed the proximal, Cys87, and interchange, Cys82 thiols with respect to the flavin, these cysteine residues function to facilitate electron movement from the flavin to the substrate, 2-ketopropyl-CoM (2-KPC). The novelty of 2-KPCC is highlighted by the subsequent cleavage of a thioether bond, formation of an enolacetone intermediate, and carboxylation of the substrate (7).

Previous studies have shown that neither the C87A nor the C82A 2-KPCC mutants have any catalytic activity with respect to the redox dependent reactions of 2-KPCC (Wampler, unpublished). As these two cysteine residues are proposed to serve purely a redox role in catalysis, it was as expected that neither of the mutations had any effect on the redox independent activity of 2-KPCC, although interestingly, the redox independent catalyzed rate enhancement of acetoacetate decarboxylation was increased with respect to the wild type enzyme.

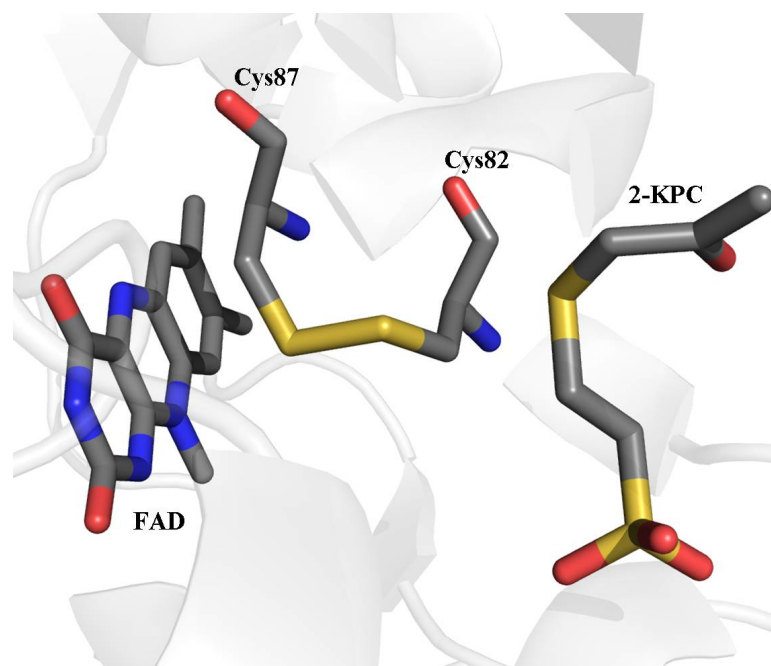


Figure 3-1. Active site of 2-KPCC with substrate bound. Electrons are transferred from the FADH to reduce the disulfide bond between Cys87 (flavin thiol) and Cys82 (interchange thiol). The mechanism of 2-KPCC proceeds by a mixed disulfide formed between Cys82 and the thiol of CoM in 2-KPC.

It is hypothesized that the thioether bond cleavage requires the thiol distal to the flavin to form a mixed disulfide bond with the thiol of CoM (7). Although this chemistry may seem unlikely, this hypothesis is supported by a crystal structure with the trapped interchange thiol-CoM mixed disulfide intermediate (13) and previous studies with the C82A mutant and with protein that had been modified by the alkylating agent, 2-bromoethanesulfonate (6).

2-bromoethanesulfonate (BES) has been shown to be an inhibitor of growth of *X. autotrophicus* on short-chain alkenes, but not propane, acetone or n-propanol, which are metabolized using CoM-independent pathways. The utility of BES as a specific inhibitor of alkene oxidation in *X. autotrophicus* by acting as a CoM analog, has indicated that it may be a useful probe to potentially identify other alkene utilizing bacteria or even other

classes of CoM utilizing bacteria in addition to the ones currently known. In addition, the identification of BES as a specific alkylating agent of the interchange thiol of 2-KPCC has been utilized to further investigate the novel features of the active site of 2-KPCC.

With the exception of the bound water molecule and coordinating histidine residues the remainder of the active site cavity is highly hydrophobic, which is believed to contribute to the preferential carboxylation of the substrate (12). In contrast to other DSOR members, which have a conserved histidine residue in close proximity of the interchange thiol, stabilizing it in the reduced state, 2-KPCC has instead a phenylalanine residue. This presence of a hydrophobic residue is thought to aid in eliminating the availability of protons to the enolacetone intermediate formed and concurrently increases the pK_a of the nearby cysteine residues with respect to other DSOR members.

The spectral features of FAD provide a valuable tool to examine the interaction of the flavin with the proximal catalytic cysteine residue Cys87 (15). When the proximal cysteine is in the thiolate form, a broad flavin-thiol charge transfer absorbance can be detected with a λ_{max} at 555 nm. Early studies of 2-KPCC utilized stopped flow spectroscopy and while a tremendous amount of knowledge was acquired from this work, some of the intermediate steps occurred too quickly to obtain spectral data (16). In these studies, two methods were used, mutation of the interchange thiol (Cys82) to an alanine, and alkylation of the interchange thiol by the inhibitor 2-bromoethanesulfonate (BES) to trap the proximal thiol in the reduced state, allowing the flavin-thiol charge transfer to be more easily observed. These modifications to 2-KPCC, along with spectral analysis were used to approximate the pK_a of the flavin thiol to be approximately 8.75, in stark contrast

to the pK_a 's determined for typical members of the DSOR family such as glutathione reductase, and lipoamide dehydrogenase.

METHODS

Materials. Commercially available compounds used were of analytical grade and purchased from either Sigma-Aldrich Chemicals or Fisher Scientific. 2-(2-Keto-propylthio)ethanesulfonate (2-KPC) was synthesized as described previously (2). All oligonucleotides were purchased from Integrated DNA Technologies.

Site Directed Mutagenesis. Site directed mutagenesis of pDW1 was carried out utilizing the Quikchange[®] Site Directed Mutagenesis Kit (Stratagene) according to the manufacturer's protocols. The sequences of the primer pairs used to create the desired mutations are as follows: C82A, 5'-TCC TGG GCG GCT CGG CCC CGC ACA ATG CGT-3' and 5'-AAG GAC CCG CCG AGC CGG GGC GTG TTA CGC-3'; C87A 5'-GTG CCC GCA CAA TGC GGC CGT GCC GCA CCA TAT GTT-3' and 5'-GAA CAG ATG GTG CGG CAC GGC CGC ATT GTG CGG GCA-3'. Mutations were confirmed by primer extension sequencing at SeqWright DNA Technology Services (Houston, TX).

Growth Media. *E. coli* Top10 cells were grown in Luria-Bertani Rich (LB-Rich) broth containing ampicillin (100 μ g/mL). The LB-Rich media contained the following components per liter: 20 g of tryptone, 15 g of yeast extract, 2 g of K_2HPO_4 , 1 g of KH_2PO_4 , and 8 g of NaCl.

Growth of Bacteria. All bacteria were grown at 37°C. *E. coli* Top10 cells that had been transformed with the pDW1 or corresponding mutant plasmid were plated and grown overnight. A single colony from this plate was used to grow a 25 mL liquid

culture to an A_{600} of 0.6 for preparation of 25% glycerol (v/v) stocks that were stored at -80°C until use. For use, cells from a frozen stock were inoculated into 125 mL of LB-Rich media and grown to an A_{600} between 0.6 and 1.0. This culture was used as the inoculum for a 15 L capacity microferm fermentor (New Brunswick Scientific) containing 12 L of LB-Rich media supplemented with riboflavin (15 mg/L) and antifoam A (0.005% v/v). Cells were allowed to grow at 37°C with stirring at 400 rpm and forced aeration to an A_{600} between 0.6 and 1.0. At this time, the temperature was reduced to 30°C , arabinose was added to 0.02% and the cells were allowed to grow at this temperature for 6 h. Cells were concentrated using a tangential flow filtration system (Millipore) and pelleted by centrifugation. Cell paste was drop frozen in liquid nitrogen and stored at -80°C .

Purification of recombinant 2-KPCC. Cell paste was resuspended in 3 volumes of buffer A (50 mM Tris, 1 mM DTT, 0.1 mM EDTA, 5% glycerol v/v) with DNase I (0.03 mg/mL) and lysozyme (0.03 mg/mL) and thawed at 30°C with shaking. All subsequent treatments were performed either on ice or at 4°C . Cell suspension was passed three times through a French pressure cell (16000 psi) and clarified by centrifugation (184000 RCF). Clarified cell extract was applied to a 0.5 x 5.0 cm column of Ni-NTA Superflow (Pharmacia Biotech) at 7.0 mL/min. The column was then washed with 4 column volumes of buffer A and the bound sample was eluted with a 15 column volume gradient from 0-400 mM imidazole. The purification was followed using SDS-PAGE analysis. Appropriate fractions were pooled and $(\text{NH}_4)_2\text{SO}_4$ was added to 800 mM. The solution was incubated at 4°C with gentle stirring and then applied to a 2.6 x 5.5 cm column of phenyl sepharose that had been equilibrated with buffer C (buffer A + 800 mM

(NH₄)₂SO₄). The column was then washed with 4 column volumes buffer C and bound protein was eluted with a 15 column volume gradient from 0-100% buffer A followed by an additional five column volumes buffer A. Appropriate fractions were pooled and concentrated by ultrafiltration using a YM30 membrane (Amicon) and frozen dropwise in liquid nitrogen for storage at -80°C.

Protein Concentration Determination. 2-KPCC concentrations were determined by using the previously determined extinction coefficient (ϵ_{450} of 11828 M⁻¹•cm⁻¹) (3).

SDS-PAGE Procedures. SDS-PAGE (12% T) was performed following the Laemmli procedure (11). Electrophoresed proteins were visualized by staining with Coomassie blue. The apparent molecular masses of polypeptides were determined by comparison with R_f values of standard proteins.

Acetoacetate Decarboxylation Assay. Assays were performed as described previously (7). Assays were conducted in 9 mL sealed serum vials with a total reaction volume of 1 mL. Vials were depleted of carbonate species by including a KOH-containing trap as described previously (8). Each assay contained 250 mM acetoacetate and 5 mM CoM in 100 mM Tris buffer, pH 7.4. Assay vials were incubated in a 30°C shaking water bath and assays were initiated by addition of 0.125 mg 2-KPCC. Acetone was quantified by gas chromatography as described previously (8).

Incubation of 2-KPCC with BES. Samples of 2-KPCC (3.6 mg/ml) were incubated anoxically as previously described in the presence of 10 mM DTT and 10 mM BES for four hours (6). At that time, the samples were desalted into 2 ml using prepacked columns of Sephadex G-25 (Pharmacia, PD-10) equilibrated in 50 mM

glycine-tris-phosphate buffer at pH 7, 9 or 11. Desalted samples were air oxidized for 30 minutes. The concentrations were normalized by extracting and quantifying FAD using sodium dodecyl sulfate as described by Aliverti and co-workers (1).

UV/Vis spectral analysis of 2-KPCC. Spectra were recorded on a Shimadzu UV-2401PC spectrophotometer.

Determination of Cys87 pK_a . All absorbance readings were obtained in a quartz untramicro (120 μ l) cuvette with black sides and a 1 cm lightpath. Aliquoted GTP buffer was adjusted to the desired pH, and 2-KPCC was added to 130 μ l of buffer. Absorbance values at 555 nm and 450 nm were then obtained using a Shimadzu UV160U UV-Vis recording spectrophotometer, interfaced with a PC running PC160 Personal Spectroscopy Software Version 1.4. The reference cell contained protein free GTP buffer. The actual pH of each solution used to obtain a spectrum was determined by mixing an appropriate amount of protein free buffer A with the each of the GTP buffers.

Data Analysis. The pK_a of the flavin cysteine residue was determined by fitting A_{555} data to a four parameter sigmoidal equation, $y = y_0 + (a/(1 + \exp(-(x-x_0)/b)))$ using the software SigmaPlot.

RESULTS

Redox-independent reactions of C82A and C87A 2-KPCC. Acetoacetate decarboxylation is a thermodynamically favorable process that occurs spontaneously, however, 2-KPCC, in the presence of CoM, has been shown to catalytically enhance the rate of acetoacetate decarboxylation (7). Unlike the physiological reaction of 2-KPC cleavage and carboxylation, 2-KPCC catalyzed acetoacetate decarboxylation is

independent of a redox active cofactor. As the role of Cys82 and Cys87 is to shuttle electrons from FADH to the substrate, it is not surprising that mutation of these residues had no negative effect on the redox independent rate of acetoacetate decarboxylation. What is more intriguing is that, both the C82A and C87A mutants had increased acetoacetate decarboxylation activity as compared to the wild type protein (Figure 3-2).

The activities of C82A and C87A 2-KPCC were 204% and 181%, respectively, of that of the wild type protein. One explanation may be that the replacement of the cysteine residues with alanine residues creates a larger binding pocket and perhaps allows for easier active site access by acetoacetate.

UV-Vis spectral analysis of BES-alkylated 2-KPCC and C82A 2-KPCC. A distinguishing feature of DSOR enzymes is the formation of a charge transfer complex that forms between the oxidized flavin and the deprotonated flavin thiolate, Cys87 in 2-KPCC. Typically the formation and disappearance of this charge transfer occurs too quickly to be easily observed, due to the tendency of the flavin thiolate to reform a disulfide bond with the interchange thiol, in this case Cys82. The charge transfer absorbance can be more readily observed upon alteration of the interchange thiol to a non-thiol containing residue or by alkylation of the interchange thiol preventing reformation of the disulfide bond. 2-bromoethanesulfonate (BES) has been shown to be an inhibitor of 2-KPCC and a selective alkylating agent of Cys82. To demonstrate this, 2-KPCC was incubated in the presence of DTT, with or without BES. The protein was desalted using gel filtration chromatography into buffer at varying pH and allowed to air oxidize before being subjected to UV-Vis spectral analysis.

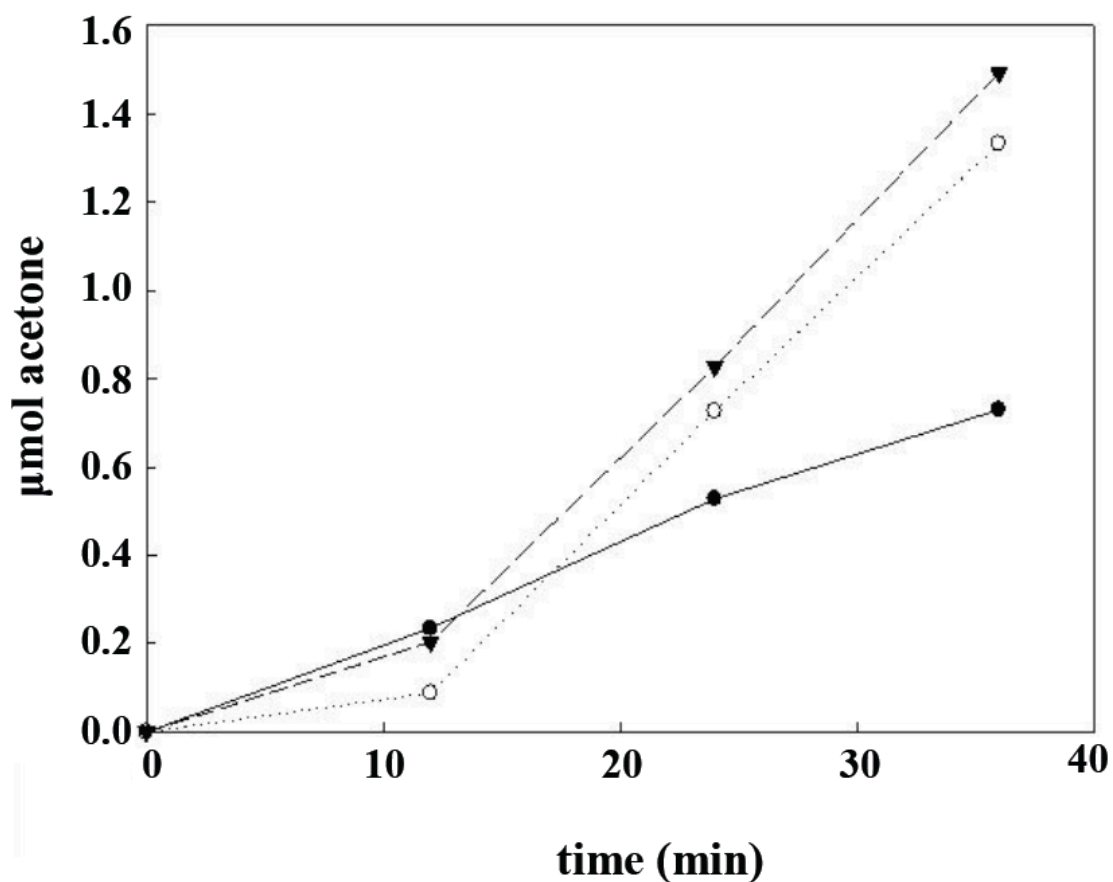


Figure 3-2. Acetone production as a result of 2-KPCC catalyzed acetoacetate decarboxylation. Assays were performed in duplicate and contained the standard assay mixture as described in Methods. Assays contained 0.125 mg 2-KPCC: ●, wild type 2-KPCC; ○, C87A 2-KPCC; ▼, C82A 2-KPCC.

As shown in Figure 3-3, 2-KPCC that had been incubated without BES showed the normal oxidized flavin spectra, while 2-KPCC that had been incubated in the presence of BES showed an increase in absorbance at A_{555} and a slightly blue shifted peak at A_{450} at pH 11, spectral features characteristic of a charge-transfer complex. Spectra of both normal 2-KPCC and BES-modified 2-KPCC that had been reduced with 1 mM dithionite

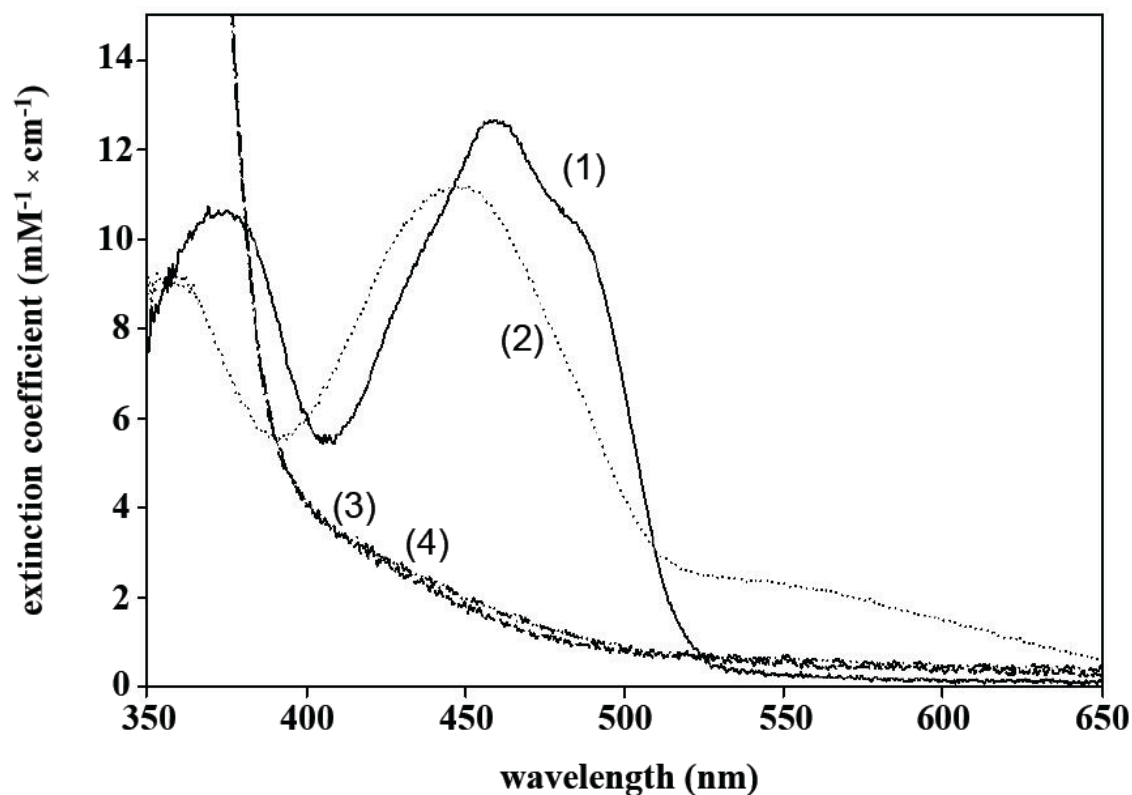


Figure 3-3. UV-visible spectra of untreated 2-KPCC and BES-modified 2-KPCC. Samples were prepared as described in Materials and Methods. The reduced spectra were obtained after removal of oxygen and the addition of 1 mM dithionite. *Trace 1*, air oxidized 2-KPCC; *trace 2*, air oxidized 2-KPCC modified by BES; *trace 3*, dithionite reduced 2-KPCC; *trace 4*, dithionite reduced 2-KPCC modified by BES.

were nearly identical, indicating spectral changes were due only to the modification of the interchange thiol. Similar results have been obtained with the C82A 2-KPCC mutant.

What is most interesting is that a pH of greater than 9 was required in order to observe the optimal charge transfer spectrum in either the C82A mutant or the BES modified protein. Spectra were obtained from BES modified 2-KPCC at a pH of 7.0, 9.0, and 11.0 (Figure 3-4).

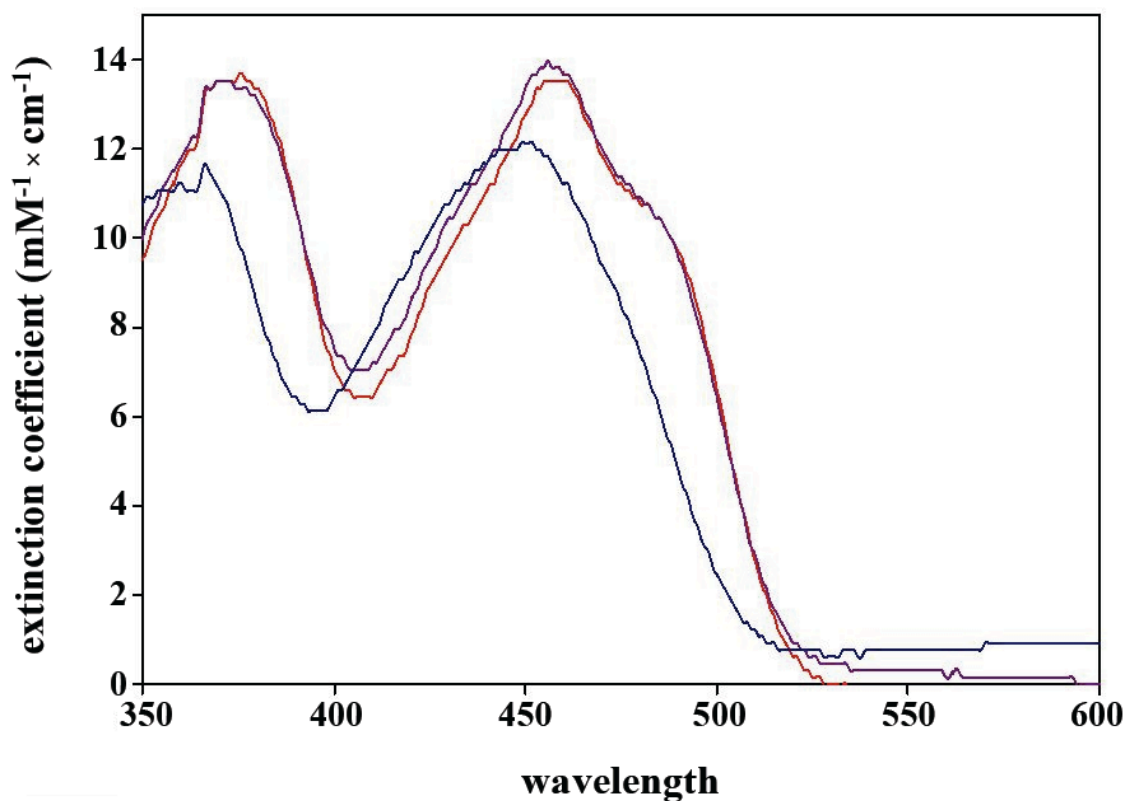


Figure 3-4. UV-visible spectra of BES modified 2-KPCC at varying pH showing the development of spectral charge transfer characteristics as a function of increasing pH. 2-KPCC samples were prepared as described in Materials and Methods. *Trace 1 (red)*, BES-modified 2-KPCC at pH 7; *trace 2 (purple)*, BES-modified 2-KPCC at pH 9; *trace 3 (blue)*, BES-modified 2-KPCC at pH 11.

At pH 7.0, the alkylated protein retains the same spectra as that of wild type 2-KPCC. At a pH of 9.0, the spectral changes characteristic of the formation of a charge transfer complex can begin to be observed. The complete spectral changes associated with the charge transfer complex cannot be visualized until pH 11.0. This is in stark contrast to other more classical DSOR members in which the charge transfer absorbance can be seen at much lower pH, for example, in the case of mercuric reductase, alkylated by

iodoacetamide, where the spectral changes can be seen at a pH of 7.4 (9), and indicates a higher pK_a for the flavin thiol in 2-KPCC than in other DSOR enzymes.

Determination of the pK_a of Cys87. The charge-transfer absorbance spectral changes, primarily the increase in A_{555} , occurs only when the flavin thiol is in the unprotonated thiolate form, and hence provides a unique tool to determine the pK_a of Cys87. Samples of 2-KPCC that had been preincubated with BES and then desalted using gel filtration chromatography were mixed with 200 mM GPT buffer at varying pH, ranging from pH 6-12 and the absorbance at A_{555} was measured. The data was then fit to a four parameter sigmoidal equation to calculate a pK_a of 8.76 ± 0.09 for Cys87. Similar analysis using the C82A 2-KPCC mutant gave a nearly identical pK_a of 8.74 ± 0.13 .

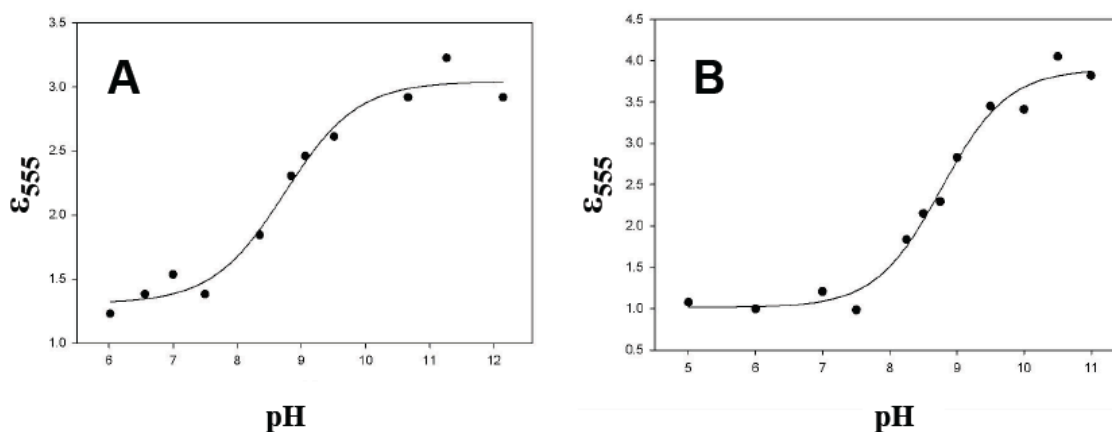


Figure 3-5. Determination of the pK_a of Cys87. The absorbance values of 2-KPCC were measured and plotted as a function of increasing pH as described in Materials and Methods. The data points were fit to a four parameter sigmoidal equation for pK_a determination. *A*, BES-modified 2-KPCC; *B*, Cys82Ala 2-KPCC.

This value varies significantly with the pK_a values for the archetypal DSOR members glutathione reductase, 4.8 (4) and mercuric ion reductase, 5.2 (14), and is most likely a result of the

unique, predominantly hydrophobic architecture of the active site of 2-KPCC. A significant contributor to this hydrophobicity is the substitution of a phenylalanine residue in 2-KPCC for the conserved histidine residue seen in other DSOR enzyme active sites (Figure 3-6) (5).

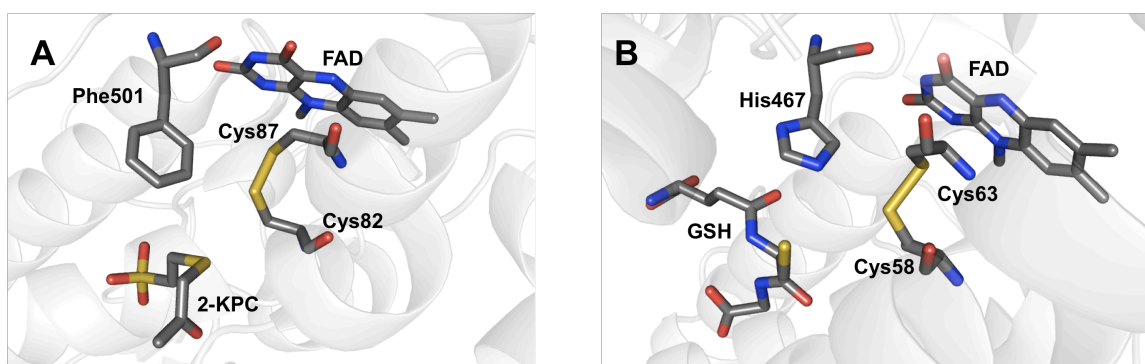


Figure 3-6. Comparison of the active sites of 2-KPCC and glutathione reductase. A, 2-KPCC active site with a phenylalanine residue in the position of a conserved histidine residue in other DSOR members; B, glutathione reductase (PDB ID: 3DK4) showing the conserved histidine residue typical of DSOR enzymes.

DISCUSSION

In these studies two different methods were utilized to further the investigation into the unique active site of 2-KPCC. Site-directed mutagenesis was used to complete the characterization of the two active site cysteine residues, Cys87 and Cys82 with respect to the redox independent reaction catalyzed by 2-KPCC, acetoacetate

decarboxylation. Both of the cysteine mutants had activity higher than the wild type protein with regard to this reaction, these results have also been seen in 2-KPCC with other active site mutations. The C82A mutation also allowed the previously undetermined pK_a of the flavin thiol of 2-KPCC, Cys87. This result was confirmed by similar analysis using 2-KPCC that had been selectively alkylated at the Cys82 position by the modifying agent and CoM analog, BES. Both modified proteins gave nearly exact values for the pK_a of Cys87. The higher pK_a value for Cys87, as opposed to the pK_a values for other DSOR enzymes, is also supported by the observation that the enzyme has optimal activity at pH 8.2 (7), a much higher pH than is typical for DSOR enzymes.

BES has been shown to be a specific inhibitor of bacterial short chain alkene metabolism, having no effect on the same bacteria grown on different substrates such as isopropanol or propane, in addition to inhibiting the growth of methanogens. There is a broad utility for BES to act as an environmental probe to potentially identify and characterize not only CoM-dependent alkene-oxidizing bacteria but also new classes of CoM utilizing bacteria in addition to the already known methanogens and alkene oxidizers.

Although BES has been shown to be an inhibitor of enzymes involved in the last two steps in the epoxide carboxylase pathway, it irreversibly inhibits only 2-KPCC and neither *R*- or *S*-HPCDH. The specificity of BES alkylation of only the interchange thiol in 2-KPCC gives BES a more specific function in the utility of it as a mechanistic probe, providing additional insight into the unique active site of this unconventional DSOR member.

REFERENCES

1. **Aliverti, A., B. Curti, and M. A. Vanoni.** 1999. Flavoprotein protocols. Humana Press, Totowa, NJ.
2. **Allen, J. R., D. D. Clark, J. G. Krum, and S. A. Ensign.** 1999. A role for coenzyme M (2-mercaptoethanesulfonic acid) in a bacterial pathway of aliphatic epoxide carboxylation. Proc. Natl. Acad. Sci. USA **96**:8432-8437.
3. **Allen, J. R., and S. A. Ensign.** 1997. Characterization of three protein components required for functional reconstitution of the epoxide carboxylase multienzyme complex from *Xanthobacter* strain Py2. J. Bacteriol. **179**:3110-3115.
4. **Arcott, L. D., C. Thorpe, and C. H. J. Williams.** 1981. Glutathione reductase from yeast. Differential reactivity of the nascent thiols in two-electron reduced enzyme and properties of a monoalkylated derivative. Biochemistry **20**:1513.
5. **Berkholz, D. S., H. R. Faber, S. N. Savvides, and P. A. Karplus.** 2008. Catalytic cycle of human glutathione reductase near 1 Å resolution. J. Mol. Biol. **382**:371-384.
6. **Boyd, J. M., D. D. Clark, M. A. Kofoed, and S. A. Ensign.** 2010. Mechanism of inhibition of aliphatic epoxide carboxylation by the coenzyme M analog 2-bromoethanesulfonate. J. Biol. Chem. **285**:25232-25242.

7. **Clark, D. D., J. R. Allen, and S. A. Ensign.** 2000. Characterization of five catalytic activities associated with the NADPH:2-ketopropyl-coenzyme M [2-(2-ketopropylthio)ethanesulfonate] oxidoreductase/carboxylase of the *Xanthobacter* strain Py2 epoxide carboxylase. *Biochemistry* **39**:1294-1304.
8. **Clark, D. D., and S. A. Ensign.** 1999. Evidence for an inducible nucleotide-dependent acetone carboxylase in *Rhodococcus rhodochrous* B276. *J. Bacteriol.* **181**:2752-2758.
9. **Fox, B. S., and C. T. Walsh.** 1983. Mercuric reductase: homology to glutathione reductase and lipoamide dehydrogenase. Iodoacetamide alkylation and sequence of the active site peptide. *Biochemistry* **22**:4082-4088.
10. **Ghisla, S., and V. Massey.** 1989. Mechanisms of flavoprotein-catalyzed reactions. *Eur. J. Biochem.* **181**:1-17.
11. **Laemmli, U. K.** 1970. Cleavage of structural proteins during the assembly of the head of bacteriophage T4. *Nature* **227**:680-685.
12. **Nocek, B., S. E. Jang, M. S. Jeong, D. D. Clark, S. A. Ensign, and J. W. Peters.** 2002. Structural basis for CO₂ fixation by a novel member of the disulfide oxidoreductase family of enzymes, 2-ketopropyl-coenzyme M oxidoreductase/carboxylase. *Biochemistry* **41**:12907-12913.
13. **Pandey, A. S., B. Nocek, S. A. E. D. D. Clark, and J. W. Peters.** 2006. Mechanistic implications of the structure of the mixed-disulfide intermediate of the disulfide oxidoreductase, 2-ketopropyl-coenzyme M oxidoreductase/carboxylase. *Biochemistry* **45**:113-120.

14. **Schultz, P. G., K. G. Au, and C. T. Walsh.** 1985. Directed mutagenesis of the redox-active disulfide in the flavoenzyme mercuric ion reductase. *Biochemistry* **24**:6840-6848.
15. **Walsh, C.** 1979. *Enzymatic reaction mechanisms.* W. H. Freeman and Co., New York.
16. **Westphal, A. H., J. Swaving, L. Jacobs, and A. de Kok.** 1998. Purification and characterization of a flavoprotein involved in the degradation of epoxyalkanes by *Xanthobacter* Py2. *Eur. J. Biochem.* **257**:160-168.

CHAPTER 4

BROMOPROPANESULFONATE AS AN INHIBITOR OF GROWTH IN
XANTHOBACTER AUTOTROPHICUS STRAIN PY2 AND AN INHIBITOR AND
SELECTIVE ALKYLATING AGENT OF 2-KPCC

ABSTRACT

The metabolism of epoxides in the bacteria *Xanthobacter autotrophicus* strain Py2, requires the atypical cofactor CoM, thought previously to be utilized only by methanogens. The CoM analog, 2-bromoethanesulfonate (BES) has been shown to be an inhibitor of growth of both methanogens and alkene oxidizing bacteria, the latter by acting as a suicide substrate and specifically and irreversibly alkylating and inactivating the last enzyme in the *X. autotrophicus* epoxide metabolism pathway, NADPH:2-ketopropyl-CoM oxidoreductase/carboxylase (2-KPCC) a member of the disulfide oxidoreductase (DSOR) family. BES inhibition of 2-KPCC occurs by specific alkylation of the interchange thiol leaving the cysteine residue modified by an ethylsulfonate group. In these studies, 3-bromopropanesulfonate (BPS) has been shown to be an even more potent inhibitor of *X. autotrophicus* growth and of the enzyme 2-KPCC, presumably because the alkylation of the interchange cysteine residue more closely resembles the normal interchange thiol-CoM mixed disulfide formed during catalysis. The concentration of BPS required for complete inhibition of *X. autotrophicus* growth was less than 75 μM , close to two orders of magnitude lower than the concentration of BES required for growth inhibition. Over short time courses, BPS exhibited competitive

inhibition of 2-KPCC with a $K_i = 34.9 \pm 8.4 \mu\text{M}$, which was also two orders of magnitude lower than the K_i determined for BES.

INTRODUCTION

The bacterial metabolism of epoxides formed from short chain aliphatic alkene epoxidation occurs by a three step, four enzyme pathway that uses the atypical cofactor coenzyme M (CoM) to facilitate epoxide ring opening and as a carrier of intermediates through the pathway. Before the discovery of CoM in *Xanthobacter autotrophicus*, the only known function of CoM was of a methyl group carrier in archaeal methanogenesis (14). 2-bromoethanesulfonate, a CoM analog, has previously been shown to be an inhibitor of both methanogenesis in archaea as well as aliphatic epoxide carboxylation in bacteria (3, 4, 9, 19). While the inhibition of these two pathways by a CoM analog may not be in itself surprising, what is interesting is that the mechanism of inhibition varies substantially between the enzymes inhibited in the aforementioned pathways. In methanogens, the target of BES is methyl CoM reductase (MCR). BES binds as a CoM analog and inactivates the enzyme by oxidizing the nickel tetrapyrrole cofactor from the +1 to +2 oxidation state (8). In bacterial epoxide metabolism, BES has been shown to be a mixed rapid equilibrium inhibitor of enzymes catalyzing the last two steps in the pathway, *R*-hydroxypropyl-CoM dehydrogenase (*R*-HPCDH) and NADPH:2-ketopropyl-CoM oxidoreductase/carboxylase (2-KPCC) (3). In addition, BES has been shown to be a time-dependent, irreversible inactivator of the terminal enzyme in the pathway, 2-KPCC, via selective alkylation of an active site cysteine residue (3).

As a member of the disulfide oxidoreductase (DSOR) family of enzymes, 2-KPCC reflects all of the notable features of this family. A flavin containing enzyme, 2-KPCC uses NADPH to reduce the bound flavin, which in turn reduces a redox active disulfide to free thiols designated as the flavin thiol and the interchange thiol. But 2-KPCC is a unique member of the DSOR family with regard to many aspects. Conventional members of the DSOR family, such as glutathione reductase and dihydrolipoamide dehydrogenase catalyze disulfide bond cleavage, forming a temporary mixed disulfide between the interchange thiol and the substrate molecule (10, 17). In contrast, 2-KPCC catalyzes the thioether bond cleavage of 2-ketopropyl-CoM (2-KPC) forming a mixed disulfide between the interchange thiol and CoM (16). The mechanism of BES inhibition in 2-KPCC has been shown to be by irreversible alkylation of the interchange thiol when the enzyme is in the reduced form. The selectivity of BES as an alkylating agent is due to the interaction of the sulfonate group with the two arginine residues that have been shown to coordinate the sulfonate group of the native substrate, 2-KPC (15).

Although the free BES molecule is an excellent CoM analog, the debrominated ethyl sulfonate bound to the enzyme is an alkyl group shorter than the mixed disulfide normally formed by CoM (Figure 4-1). It is reasonable to assume that 3-bromopropanesulfonate (BPS) may be a better CoM mimic when bound to the interchange thiol of 2-KPCC. BPS has also been shown to be an even more potent inhibitor of MCR, also by oxidizing the nickel tetrapyrrole cofactor, but by a different mechanism than BES (8, 11, 12).

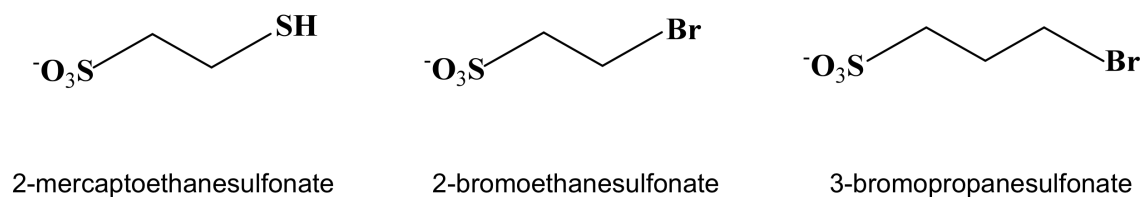


Figure 4-1. Comparative structures of 2-mercaptoethanesulfonate (CoM), 2-bromoethanesulfonate (BES) and 2-bromopropanesulfonate (BPS).

Based on the studies of BES inhibition in bacterial epoxide metabolism, and BPS inhibition in methanogens, BPS was studied as a potential inhibitor of epoxide metabolism in *X. autotrophicus* and specifically of the last enzyme in the bacterial epoxide degradation pathway, 2-KPCC. BPS has been shown to completely inhibit *X. autotrophicus* growth at a concentration of 75 μM , which is close to two orders of magnitude lower than the threshold concentration of BES, 3 mM, required to completely inhibit bacterial growth. In addition, over the course of short time frames, BPS was found to act as a competitive inhibitor of 2-KPCC with an inhibition constant also two orders of magnitude lower than that determined for BES.

METHODS

Materials. Commercially available compounds used were of analytical grade and purchased from either Sigma-Aldrich Chemicals or Fisher Scientific. 3-bromopropanesulfonate was purchased from ScienceLab, Houston, TX. 2-(2-Ketopropylthio)ethanesulfonate (2-KPC) was synthesized as described previously (1).

Growth of *X. autotrophicus* and Measurement of Cell Growth. Bacteria were grown at 30°C in a mineral salts medium (6) as described previously (18). Cultures were

grown in 50 mL of medium in sealed 250 mL shake flasks that had been modified by the addition of a Klett-compatible side arm for measuring optical densities and by replacement of the flask openings with 20 mm crimp-sealable tops and side arms for introduction of gaseous growth substrates. Cultures were inoculated with 1 mL of cells growing in log phase and with 30 mL of propylene. For the addition of BPS to cultures, a 26.7 mM stock solution was prepared and filter sterilized using a 0.2 μm acrodisc filter. BPS was then added from the stock solution so that the final concentration was 75 μM . The optical densities were determined approximately every three hours by placing the side arms of the culture flasks in a Klett-Summerson photoelectric colorimeter with a no. 66 filter. The Klett-Summerson colorimeter was standardized using a Shimadzu model UV-2101 spectrophotometer for conversion of Klett readings to absorbance values (optical density at 600 nm).

Growth of *Escherichia coli* Expressing Recombinant 2-KPCC. All *E. coli* were grown at 37°C. *E. coli* Top10 cells were grown in Luria-Bertani Rich (LB-Rich) broth containing ampicillin (100 $\mu\text{g}/\text{mL}$). The LB-Rich media contained the following components per liter: 20 g of tryptone, 15 g of yeast extract, 2 g of K_2HPO_4 , 1 g of KH_2PO_4 , and 8 g of NaCl. For the expression of 2-KPCC, *E. coli* Top10 cells that had been transformed with pDW1 were plated and grown overnight. A single colony from this plate was used to grow a 25 mL liquid culture to an A_{600} of 0.6 for preparation of 25% glycerol (v/v) stocks that were stored at -80°C until use. For use, cells from a frozen stock were inoculated into 125 mL of LB-Rich media and grown to an A_{600} between 0.6 and 1.0. This culture was used as the inoculum for a 15 L capacity microferm fermentor (New Brunswick Scientific) containing 12 L of LB-Rich media supplemented with

riboflavin (15 mg/L) and antifoam A (0.005% v/v). Cells were allowed to grow at 37°C with stirring at 400 rpm and forced aeration to an A_{600} between 0.6 and 1.0. At this time, the temperature was reduced to 30°C, arabinose was added to 0.02% and the cells were allowed to grow at this temperature for 6 h. Cells were concentrated using a tangential flow filtration system (Millipore) and pelleted by centrifugation. Cell paste was drop frozen in liquid nitrogen and stored at -80°C.

Purification of recombinant 2-KPCC. Cell paste was resuspended in 3 volumes of buffer A (50 mM Tris, 1 mM DTT, 0.1 mM EDTA, 5% glycerol v/v) with DNase I (0.03 mg/mL) and lysozyme (0.03 mg/mL) and thawed at 30°C with shaking. All subsequent treatments were performed either on ice or at 4°C. Cell suspension was passed three times through a French pressure cell (16000 psi) and clarified by centrifugation (184000 RCF). Clarified cell extract was applied to a 0.5 x 5.0 cm column of Ni-NTA Superflow (Pharmacia Biotech) at 7.0 mL/min. The column was then washed with 4 column volumes of buffer A and the bound sample was eluted with a 15 column volume gradient from 0-400 mM imidazole. The purification was followed using SDS-PAGE analysis. Appropriate fractions were pooled and $(\text{NH}_4)_2\text{SO}_4$ was added to 800 mM. The solution was incubated at 4°C with gentle stirring and then applied to a 2.6 x 5.5 cm column of phenyl sepharose that had been equilibrated with buffer C (buffer A + 800 mM $(\text{NH}_4)_2\text{SO}_4$). The column was then washed with 4 column volumes buffer C and bound protein was eluted with a 15 column volume gradient from 0-100% buffer A followed by an additional five column volumes buffer A. Appropriate fractions were pooled and concentrated by ultrafiltration using a YM30 membrane (Amicon) and frozen dropwise in liquid nitrogen for storage at -80°C.

Protein Concentration Determination. 2-KPCC concentrations were determined by using the previously determined extinction coefficient (ϵ_{450} of $11828 \text{ M}^{-1} \cdot \text{cm}^{-1}$) (2).

SDS-PAGE Procedures. SDS-PAGE (12% T) was performed following the Laemmli procedure (13). Electrophoresed proteins were visualized by staining with Coomassie blue. The apparent molecular masses of polypeptides were determined by comparison with R_f values of standard proteins.

Coupled Spectrophotometric Assay for 2-KPCC Carboxylation Activity. A continuous spectrophotometric assay was utilized that couples acetoacetate production by 2-KPCC to acetoacetate reduction and concomitant NADH oxidation by β -Hydroxybutyrate Dehydrogenase (β -HBDH) (5). Purification of β -HBDH for use in the assay was performed as described previously (5). Assays were conducted in 2 mL anaerobic quartz cuvettes that contained a total reaction volume of 1 mL. Assays contained 0.125 mg 2-KPCC, 0.345 mg β -HBDH, 10 mM DTT, 0.2 mM NADH, 60 mM carbonate species (added as 33.5 mM CO_2 gas plus 26.5 mM KHCO_3), 0.25-5.0 mM 2-KPC and 10-200 μM BPS in 100 mM Tris buffer, pH 7.4. Reactions were allowed to equilibrate to 30°C and assays were initiated by the addition of 2-KPC and BPS, which was allowed to equilibrate in a needle before addition. Acetoacetate production by 2-KPCC and subsequent reduction by NADH was quantified by monitoring the decrease in absorbance (A_{340}) associated with the oxidation of NADH in a Shimadzu UV160U spectrophotometer containing a water-jacketed cell holder for temperature control.

Incubation of 2-KPCC with BES. Samples of 2-KPCC (2.4 mg/ml) were incubated anoxically as previously described in the presence of 10 mM DTT and 10 mM

BPS for four hours (3). At that time, the samples were desalted into 2 ml using prepacked columns of Sephadex G-25 (Pharmacia, PD-10) equilibrated in 100 mM lysine buffer with 100 mM NaCl and 0.1 mM EDTA at pH 11. Desalted samples were air oxidized for 30 minutes before being subjected to UV/Vis spectral analysis.

UV/Vis spectral analysis of 2-KPCC. Spectra were obtained on a Cary UV/Visible Bio50 spectrophotometer.

Data Analysis. Initial velocity data were plotted as velocity versus substrate concentration and fit to the standard form of the Michaelis-Menten equation as described by Cleland (7) using the software SigmaPlot 11. Enzyme inhibition data were fit to the following form of the Michaelis-Menten equation, $f = V_{max}[S]/(K_m(1 + ([I]/K_i)) + [S])$ which describes the effect of a competitive inhibitor (7).

RESULTS

Growth Inhibition of *X. autotrophicus* by BPS. Both BES and BPS have been shown to be inhibitors of methanogenesis with BPS being the more potent inhibitor of the two. BES has been shown to be an inhibitor of epoxide metabolism in two known bacteria that utilize a CoM-dependent pathway, *X. autotrophicus* and *Rhodococcus rhodochrous*. It was of interest to determine if BPS was also a more potent inhibitor of alkene oxidizing bacteria in a similar fashion to that observed in methanogens. To determine this, cultures of *X. autotrophicus* were allowed to grow in sealed flasks on propylene in the absence and presence of BPS with OD₆₀₀ readings taken every three hours. Upon the addition of 75 μM BPS, growth was completely inhibited. The concentration of BPS to be used was determined by prior growth experiments designed to

find the minimum concentration at which BPS could completely inhibit growth. To determine the specificity of BPS inhibition, *X. autotrophicus* was also grown on isopropanol, a compound that does not require CoM for metabolism, in the presence and absence of BPS. The presence of BPS had no effect on the growth of the bacteria when grown under these conditions (data not shown).

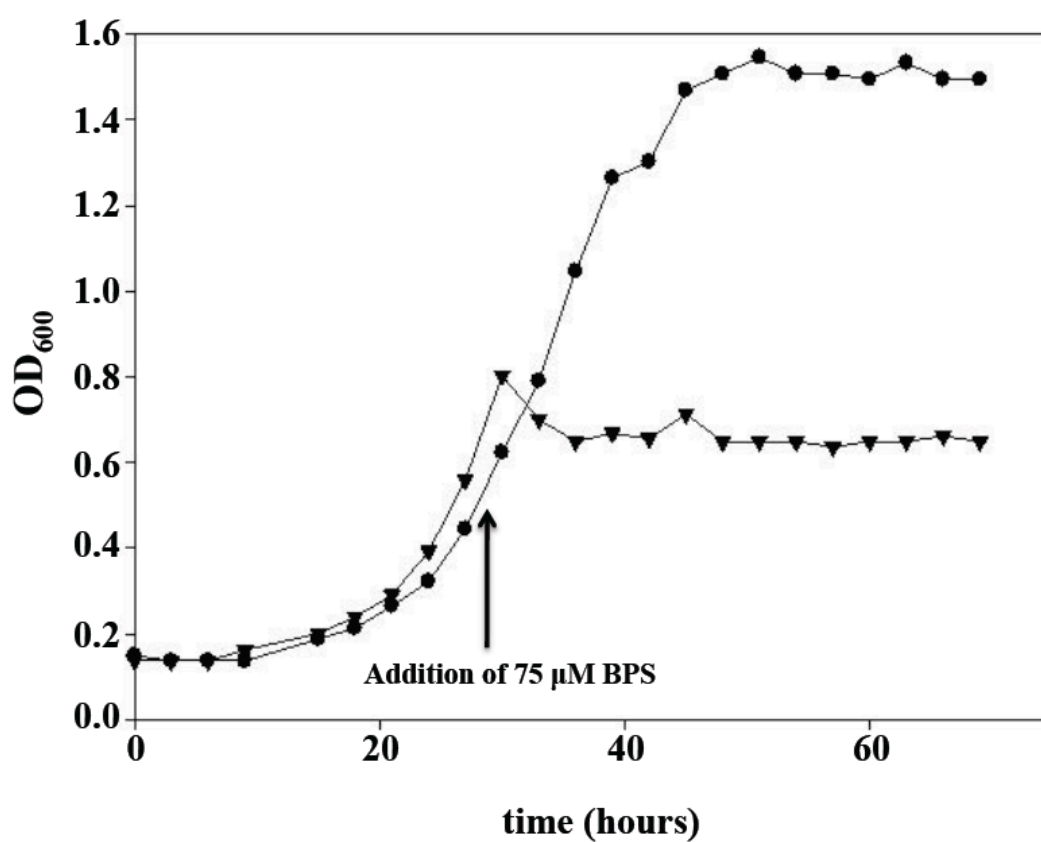


Figure 4-2. Growth of *X. autotrophicus* in the presence and absence of BPS. ●, 0 μM BPS; ▼, 75 μM BPS added at the time indicated on the graph.

Kinetic Characterization of Rapid Equilibrium Inhibition of 2-KPCC by BPS.

Previous studies have shown BES to be a rapid equilibrium inhibitor of 2-KPCC, as well as a time dependent irreversible inactivator of the enzyme. Although 2-KPCC is capable of catalyzing several different reactions, the physiologically relevant reaction catalyzed is the reductive cleavage and carboxylation of 2-KPC resulting in the formation of acetoacetate. Previous measurement of this activity required a discontinuous assay which quantified the amount of radiolabeled $^{14}\text{CO}_2$ incorporated into acetoacetate. In these studies a new, recently developed assay was utilized which couples the production of acetoacetate to the activity of β -HBDH and concomitant oxidation of NADH, which can be measured spectrophotometrically by following the decrease in A_{340} . Activity of the enzyme was monitored over short time courses (20-40 s) and the progress curves for product formation were largely linear in the absence and presence of BPS. If assays were allowed to proceed for longer time periods (longer than one minute) there was a decrease in progress curve linearity, suggesting that BPS may be a time dependent inactivator of 2-KPCC as well.

The carboxylation activity of 2-KPCC was measured as described above in the presence of varying concentrations of BPS and varying concentrations of 2-KPC, with saturating concentrations of DTT, NADH, CO_2 and β -HBDH. As shown in Figure 4-3, BPS behaved essentially as a competitive inhibitor during the short time courses of the assays. The experimental data were used to calculate the following kinetic parameters: $k_{cat} = 12.7 \text{ min}^{-1}$, $K_m = 269 \pm 56 \text{ }\mu\text{M}$, and $K_i = 34.9 \pm 8.3 \text{ }\mu\text{M}$.

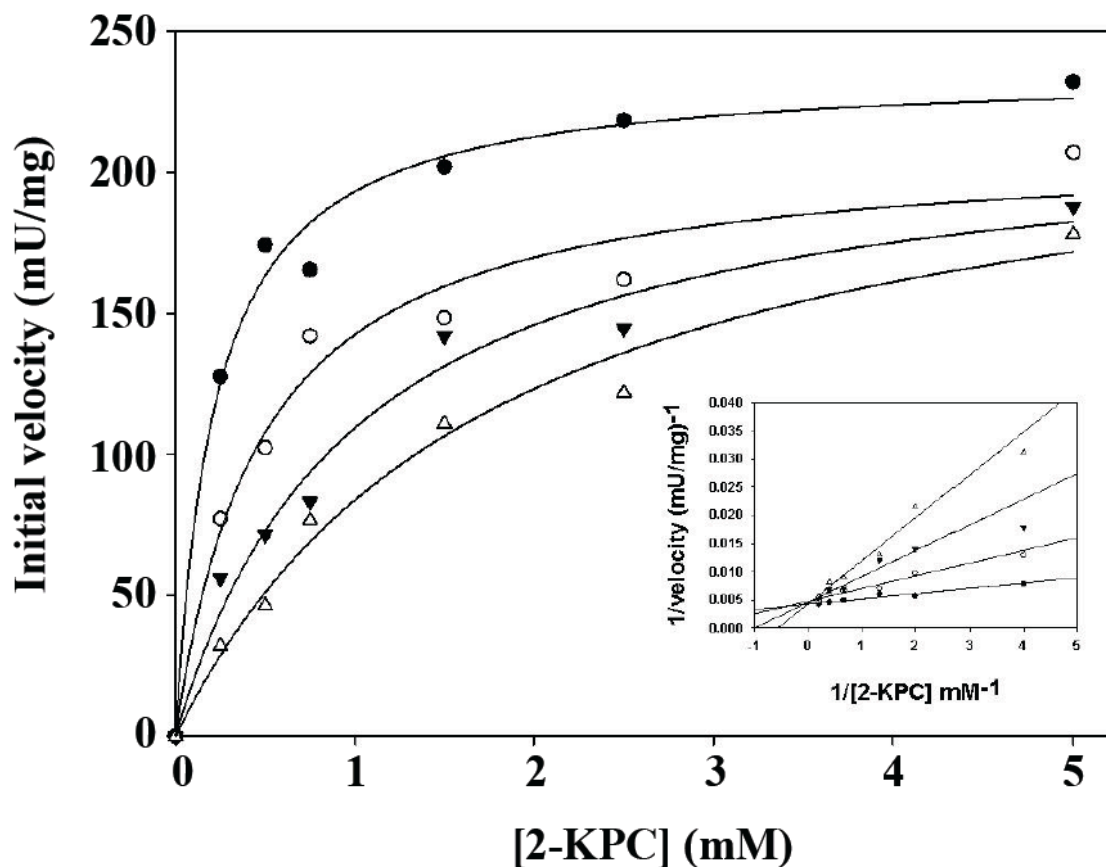


Figure 4-3. Competitive rapid equilibrium inhibition of 2-KPCC catalyzed 2-KPC oxidation by BPS. Assays of 2-KPC carboxylation were performed as described in Materials and Methods with 0.125 mg of 2-KPCC and varying concentrations of BPS. Data points represent the average of duplicate experiments and were fit to the standard form of the Michaelis-Menten equation. Symbols: ●, 0 mM BPS; ○, 10 μ M BPS; ▼, 100 μ M BPS; △, 200 μ M BPS. *Inset*, double reciprocal plots for the assays with the solid lines being generated from nonlinear least-squares fits of the velocity versus [S] data to the equation for a rectangular hyperbola using Sigmaplot.

UV-Visible Spectroscopic Evidence for Alkylation of Cys82 by BPS. As typical for all DSOR enzymes, a flavin-thiolate charge transfer complex results from the interaction of the proximal cysteine and the oxidized flavin when the proximal cysteine, Cys87 in the case of 2-KPCC, is in the deprotonated thiolate form. Usually the charge-transfer complex develops and dissipates too quickly to be easily observed. However,

upon modification of the interchange thiol, which renders the proximal thiol in a continually reduced state, the distinguishing features of the complex, most prominently an increase in absorbance around A_{555} can be easily visualized spectrophometrically. 2-KPCC that had been incubated in the presence of BPS, shows the typical spectral

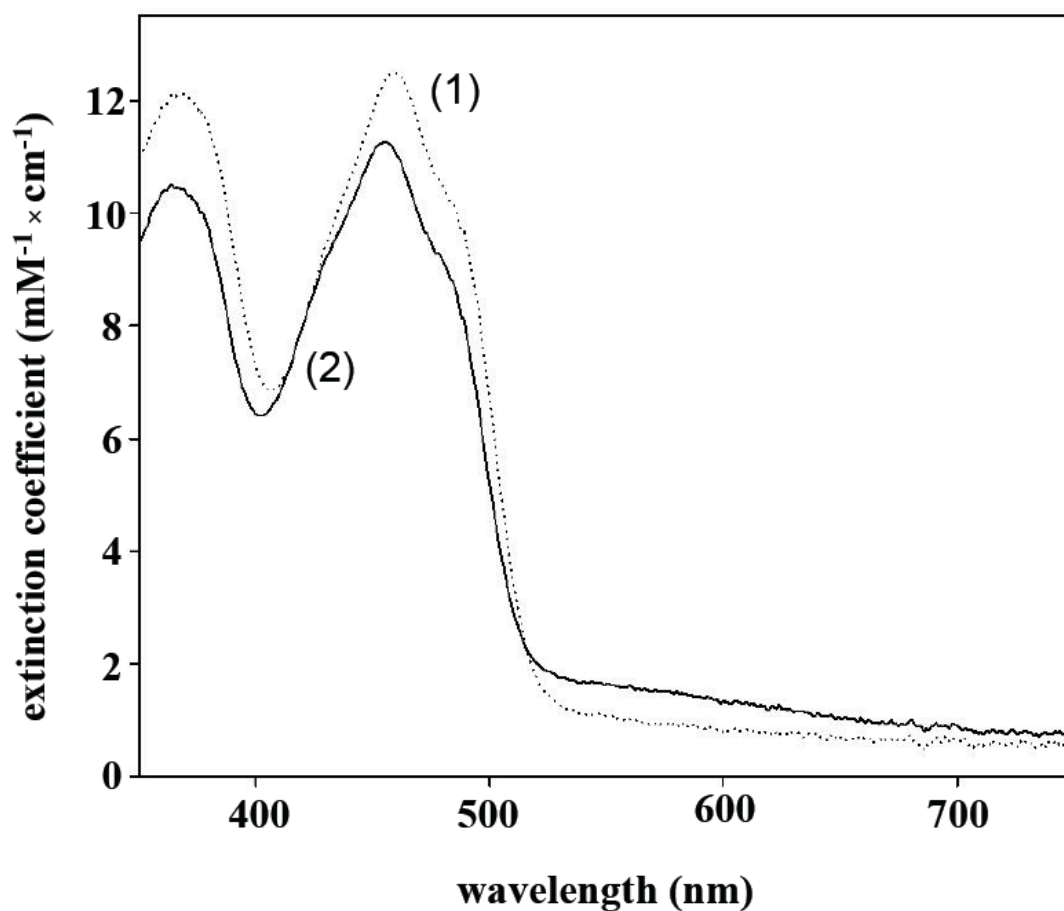


Figure 4-4. Spectral changes associated upon modification of 2-KPCC that had been alkylated by BPS. *Trace 1*, 2-KPCC that had been preincubated in the absence of BPS; *Trace 2*, 2-KPCC that had been incubated in the presence of BPS.

characteristics associated with a flavin-thiol charge transfer complex, indicating that the protein undergoes alkylation in a similar fashion to protein modified by BES which has been more extensively characterized.

DISCUSSION

The studies in this chapter have identified BPS as another and more potent inhibitor of epoxide metabolism in *X. autotrophicus*, with the target of irreversible alkylation being the final enzyme in the epoxide metabolism pathway, 2-KPCC.

BES was the initial structural CoM analog identified as an inhibitor of methanogenesis by inhibiting the methane liberating enzyme, methyl CoM reductase (MCR) with a $K_i = 2 \mu\text{M}$ (8). While BPS, also a structural analog of CoM, has been shown to be an even more potent inhibitor of methanogenesis ($K_i = 0.1 \mu\text{M}$) (8), its inhibition of MCR is by a different mechanism than BES.

The concentration of BPS at which *X. autotrophicus* growth was inhibited and the concentration at which half maximal inhibition for 2-KPCC were about 100 times lower than the concentrations of BES required. These BPS concentrations are much more similar to the inhibition constant determined for MCR in methanogens. This is most likely due to the mechanism of inhibition for BES and BPS in 2-KPCC. Both inhibitors are suicide substrates for 2-KPCC and inhibit the enzyme by irreversibly alkylating the interchange thiol, Cys82. The structure of the alkylated thiol most likely closely resembles the mixed disulfide intermediate formed between the thiol of CoM and the interchange thiol during catalysis. Due to this mechanism (Figure 4-5), with bromine serving as the leaving group, BPS is a better CoM analog after modifying Cys82. As

CoM is oriented in the active site of 2-KPCC by interaction of the sulfonate group with two arginine residues, it is reasonable to assume that the orientation of BPS in the active site, being one alkyl group longer than

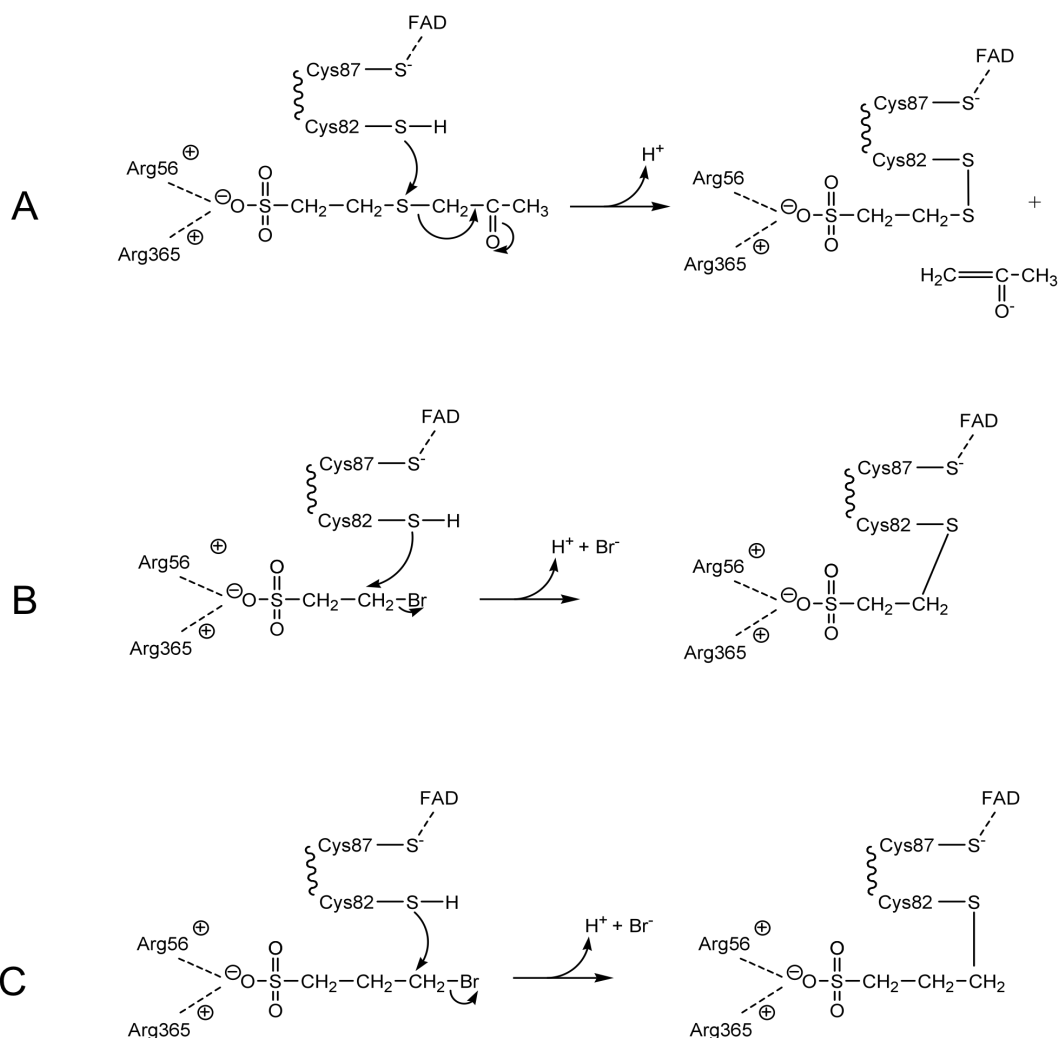


Figure 4-5. Comparison of the mixed disulfide formed in 2-KPCC during catalysis between the interchange thiol and the thiol of CoM and 2-KPCC that had been alkylated by BES or BPS at Cys82. A, Mixed disulfide intermediate formed between Cys82 and CoM; B, alkylation of Cys82 by BES; C, alkylation of Cys82 by BPS.

BES, puts the inhibitor in a conceivably better orientation for nucleophilic attack by the thiol of Cys82. This hypothesis is also supported by the observation that no inhibition was seen with other brominated compounds lacking a sulfonate group.

Further studies will investigate the time dependent irreversible inactivation of 2-KPCC by BPS. It is also planned to look at the inhibition *R*-HPCDH by BPS. Inhibition in *R*-HPCDH is presumed to be completely reversible, in a similar fashion as inhibition by BES, and the inhibition constant for this enzyme by BPS is proposed to be similar as that obtained using BES.

REFERENCES

1. **Allen, J. R., D. D. Clark, J. G. Krum, and S. A. Ensign.** 1999. A role for coenzyme M (2-mercaptoethanesulfonic acid) in a bacterial pathway of aliphatic epoxide carboxylation. *Proc. Natl. Acad. Sci. USA* **96**:8432-8437.
2. **Allen, J. R., and S. A. Ensign.** 1997. Characterization of three protein components required for functional reconstitution of the epoxide carboxylase multienzyme complex from *Xanthobacter* strain Py2. *J. Bacteriol.* **179**:3110-3115.
3. **Boyd, J. M., D. D. Clark, M. A. Kofoed, and S. A. Ensign.** 2010. Mechanism of inhibition of aliphatic epoxide carboxylation by the coenzyme M analog 2-bromoethanesulfonate. *J. Biol. Chem.* **285**:25232-25242.
4. **Boyd, J. M., A. Ellsworth, and S. A. Ensign.** 2006. Characterization of 2-bromoethanesulfonate as a selective inhibitor of the coenzyme M-dependent

- pathway and enzymes of aliphatic epoxide metabolism. *J. Bacteriol.* **188**:8062-8069.
5. **Boyd, J. M., and S. A. Ensign.** 2005. ATP-dependent enolization of acetone by acetone carboxylase from *Rhodobacter capsulatus*. *Biochemistry* **44**:8543-8553.
 6. **Clark, D. D., and S. A. Ensign.** 1999. Evidence for an inducible nucleotide-dependent acetone carboxylase in *Rhodococcus rhodochrous* B276. *J. Bacteriol.* **181**:2752-2758.
 7. **Cleland, W. W.** 1979. Statistical analysis of enzyme kinetic data. *Methods Enzymol.* **63**:103-138.
 8. **Goenrich, M., F. Mahlert, E. C. Duin, C. Bauer, B. Jaun, and R. K. Thauer.** 2004. Probing the reactivity of Ni in the active site of methyl-coenzyme M reductase with substrate analogs. *J. Biol. Inorg. Chem.* **9**:691-705.
 9. **Gunsalus, R. P., J. A. Romesser, and R. S. Wolfe.** 1978. Preparation of coenzyme M analogues and their activity in the methyl coenzyme M reductase system of *Methanobacterium thermoautotrophicum*. *J. Bacteriol.* **17**:2374-2377.
 10. **Karplus, P. A., and G. E. Schulz.** 1989. Substrate binding and catalysis by glutathione reductase as derived from refined enzyme: substrate crystal structure at 2 angstrom resolution. *J. Mol. Biol.* **210**:163-180.
 11. **Kunz, R. C., M. Dey, and S. W. Ragsdale.** 2008. Characterization of the thioether product formed from the thiolytic cleavage of the alkyl-nickel bond in methyl-coenzyme M reductase. *Biochemistry* **47**:2661-2667.

12. **Kunz, R. C., Y. C. Horng, and S. W. Ragsdale.** 2006. Spectroscopic and kinetic studies of the reaction of bromopropanesulfonate with methyl-coenzyme M reductase. *J. Biol. Chem.* **281**:34663-34676.
13. **Laemmli, U. K.** 1970. Cleavage of structural proteins during the assembly of the head of bacteriophage T4. *Nature* **227**:680-685.
14. **McBride, B. C., and R. S. Wolfe.** 1971. A new coenzyme of methyl transfer, coenzyme M. *Biochemistry* **10**:2317-2324.
15. **Nocek, B., S. E. Jang, M. S. Jeong, D. D. Clark, S. A. Ensign, and J. W. Peters.** 2002. Structural basis for CO₂ fixation by a novel member of the disulfide oxidoreductase family of enzymes, 2-ketopropyl-coenzyme M oxidoreductase/carboxylase. *Biochemistry* **41**:12907-12913.
16. **Pandey, A. S., B. Nocek, S. A. Ensign, D. D. Clark, and J. W. Peters.** 2006. Mechanistic implications of the structure of the mixed-disulfide intermediate of the disulfide oxidoreductase, 2-ketopropyl-coenzyme M oxidoreductase/carboxylase. *Biochemistry* **45**:113-120.
17. **Sahlman, L., and C. H. Williams Jr.** 1989. Titration studies on the active sites of pig heart lipoamide dehydrogenase and yeast glutathione reductase as monitored by the charge transfer absorbance. *J. Biol. Chem.* **264**:8033-8038.
18. **Small, F. J., and S. A. Ensign.** 1995. Carbon dioxide fixation in the metabolism of propylene and propylene oxide by *Xanthobacter* strain Py2. *J. Bacteriol.* **177**:6170-6175.
19. **Wolfe, R. S.** 1991. My kind of biology. *Annu. Rev. Biochem.* **45**:1-35.

CHAPTER 5

CONCLUSIONS AND FUTURE DIRECTIONS

Aliphatic alkenes and epoxides have been shown to have detrimental effects on biological organisms. However, there are some bacteria that have been shown to not only detoxify these compounds, but productively metabolize them as well. *Xanthobacter autotrophicus* and *Rhodococcus rhodochrous*, utilize a distinct pathway for epoxide metabolism that necessitates the use of the atypical cofactor Coenzyme M (CoM) (1-4, 8), contains one of only two known pairs of short chain dehydrogenases that catalyze the same reaction but with opposite stereospecificity, and concludes with an innovative strategy of substrate carboxylation.

The chapters in this dissertation have provided an in-depth look the terminal enzyme in the epoxide metabolism pathway, a carboxylase and the CoM regenerating enzyme of the pathway, and specifically at the features that make NADPH:2-ketopropyl CoM oxidoreductase/carboxylase (2-KPCC) unique as a member of the disulfide oxidoreductase (DSOR) family of enzymes. Previous hypotheses of enolate stabilization by an ordered water molecule, based on the initial studies of 2-KPCC and refined crystal structures, have now been confirmed by the analysis of two histidine mutants. The effect of the unique hydrophobic architecture of the 2-KPCC active site on the pK_a of the interchange thiol has been investigated, and the determination of the pK_a of Cys87 is shown to be significantly higher than its DSOR counterparts. The molecules 2-bromoethanesulfonate (BES) and 3-bromopropanesulfonate (BPS) have been investigated not only as inhibitors of 2-KPCC, but also as modifying agents of 2-KPCC. This provides additional insight into the active site of this novel enzyme. Detailed

investigation of these features, have provided a comprehensive picture of how 2-KPCC is capable of catalyzing the cleavage of a thioether bond and subsequent carboxylation, by a previously unprecedented mechanism.

The characterization of BPS as an inhibitor of the epoxide carboxylation pathway has not been fully investigated. Similar to BES, preliminary studies have indicated that BPS is a time-dependent inactivator of 2-KPCC in addition to being a competitive inhibitor. In contrast to the four hours required for BES to completely inactivate 2-KPCC, it appears that inactivation by BPS requires only about thirty minutes. These observations further emphasize the increased potency of BPS as an inhibitor and indicate that BPS may serve as a better environmental probe than BES to discover and identify methanogens, alkene oxidizing bacteria and other potential CoM dependent organisms.

Recent crystal structure data for 2-KPCC have identified other structural features that would be worth further investigation. One of the main structural differences between 2-KPCC and typical DSOR enzymes is the presence of a thirteen amino acid insertion flanked by two proline residues that allow tight looping of the region (5). 2-KPCC also has notable differences at both the N- and C-termini of the protein, and together these three additional regions occupy what would be the large substrate binding cleft in other members of the DSOR family. This loop not only serves to prevent solvent access to the active site but also aids in formation of the small hydrophobic channel that allows CO₂ access to the active site. It would be interesting to try to make a 2-KPCC loop deletion mutant and to observe the changes in activity and differential product formation as a result.

Besides the presence of the histidine residues comprising the catalytic triad, one of the main active site differences between 2-KPCC and other DSOR enzyme active sites is the substitution of a phenylalanine residue for a conserved histidine residue. This difference is proposed to be a reflection of the different reactions catalyzed by 2-KPCC and functions to maintain the general hydrophobicity of the active site and eliminate protons. It is the presence of this residue that is thought to be a major contributor to the basic shift of the pK_a of the Cys87. The generation of a F501H 2-KPCC mutant would have provided interesting insight into the unique active site of 2-KPCC. Unfortunately many attempts at the creation of this mutant have proven unsuccessful.

There is also a proposed alternate anion binding site composed of Gln509 and His506 that is proposed to function to stabilize the negative charge on acetoacetate formed during catalysis (6, 7). This site may also aid in acetoacetate binding in the active site during the redox independent catalyzed acetoacetate decarboxylation reaction. Again, site directed mutagenesis of these two residues could provide more information on the role of this potential alternate anion binding site.

Although there are still some questions to be answered, many of the details of 2-KPCC have been elucidated. The basis for 2-KPCC cleavage of a thioether bond and preferential carboxylation of the substrate, highlights the mechanistic versatility of DSOR enzymes and contributes to furthering the understanding of fundamental mechanisms that impart bacteria with the ability to detoxify and exploit potentially toxic compounds for productive metabolism.

REFERENCES

1. **Allen, J. R., D. D. Clark, J. G. Krum, and S. A. Ensign.** 1999. A role for coenzyme M (2-mercaptoethanesulfonic acid) in a bacterial pathway of aliphatic epoxide carboxylation. *Proc. Natl. Acad. Sci. USA* **96**:8432-8437.
2. **Allen, J. R., and S. A. Ensign.** 1996. Carboxylation of epoxides to β -Keto acids in cell extracts of *Xanthobacter* strain Py2. *J. Bacteriol.* **178**:1469-1472.
3. **Allen, J. R., and S. A. Ensign.** 1997. Purification to homogeneity and reconstitution of the individual components of the epoxide carboxylase multiprotein enzyme complex from *Xanthobacter* strain Py2. *J. Biol. Chem.* **272**:32121-32128.
4. **Ensign, S. A., F. J. Small, J. R. Allen, and M. K. Sluis.** 1998. New roles for CO₂ in the microbial metabolism of aliphatic epoxides and ketones. *Arch. Microbiol.* **169**:179-187.
5. **Nocek, B., S. E. Jang, M. S. Jeong, D. D. Clark, S. A. Ensign, and J. W. Peters.** 2002. Structural basis for CO₂ fixation by a novel member of the disulfide oxidoreductase family of enzymes, 2-ketopropyl-coenzyme M oxidoreductase/carboxylase. *Biochemistry* **41**:12907-12913.
6. **Pandey, A. S., D. W. Mulder, S. A. Ensign, and J. W. Peters.** 2011. Structural basis for carbon dioxide binding by 2-ketopropyl coenzyme M oxidoreductase/carboxylase. *FEBS Lett.* **585**:459-464.
7. **Pandey, A. S., B. Nocek, S. A. E. D. D. Clark, and J. W. Peters.** 2006. Mechanistic implications of the structure of the mixed-disulfide intermediate of

the disulfide oxidoreductase, 2-ketopropyl-coenzyme M oxidoreductase/carboxylase. *Biochemistry* **45**:113-120.

8. **Small, F. J., and S. A. Ensign.** 1995. Carbon dioxide fixation in the metabolism of propylene and propylene oxide by *Xanthobacter* strain Py2. *J. Bacteriol.* **177**:6170-6175.

APPENDIX

JOURNAL OF BIOLOGICAL CHEMISTRY COPYRIGHT GUIDELINES

Copyright Permission Policy

These guidelines apply to the reuse of articles, figures, charts and photos in the *Journal of Biological Chemistry*, *Molecular & Cellular Proteomics* and the *Journal of Lipid Research*.

For authors reusing their own material:

Authors need **NOT** contact the journal to obtain rights to reuse their own material. They are automatically granted permission to do the following:

- Reuse the article in print collections of their own writing.
- Present a work orally in its entirety.
- Use an article in a thesis and/or dissertation.
- Reproduce an article for use in the author's courses. (If the author is employed by an academic institution, that institution also may reproduce the article for teaching purposes.)
- Reuse a figure, photo and/or table in future commercial and noncommercial works.
- Post a copy of the paper in PDF that you submitted via BenchPress.
- Only authors who published their papers under the "Author's Choice" option may post the final edited PDFs created by the publisher to their own/departmental/university Web sites.
- All authors may link to the journal site containing the final edited PDFs created by the publisher.

Please note that authors must include the following citation when using material that appeared in an ASBMB journal:

"This research was originally published in Journal Name. Author(s). Title. *Journal Name*. Year; Vol:pp-pp.
© the American Society for Biochemistry and Molecular Biology."

For other parties using material for noncommercial use:

Other parties are welcome to copy, distribute, transmit and adapt the work — at no cost and without permission — for noncommercial use as long as they attribute the work to the original source using the citation above.

Examples of noncommercial use include:

- Reproducing a figure for educational purposes, such as schoolwork or lecture presentations, with attribution.
- Appending a reprinted article to a Ph.D. dissertation, with attribution.

CURRICULUM VITAE

Melissa A. Beighley-Kofoed

132 Penny Lane • Logan, UT 84341 • 563.542.0677 • missybeighley@gmail.com

EDUCATION	Utah State University	
	Ph.D, Biochemistry	April
2011		
	University of Wisconsin-Oshkosh	
	Bachelor of Science	December 2004
	Majors: Chemistry	
	Biology	

ACADEMIC EXPERIENCE

Research Assistant – Utah State University - Logan, UT	6/06-
4/11	
<ul style="list-style-type: none"> • Biochemistry research under Prof. Scott Ensign • Experience in- Microbiology, Enzymology, Molecular Biology • Proficient at the following techniques- Spectroscopy (GC, UV/Vis), protein purification, gel electrophoresis, PCR, site-directed mutagenesis, gene cloning/transformation/expression • Radiation Safety certified 	
Teaching Assistant – Utah State University – Logan, UT	
General Chemistry 1210/1220	8/05-5/06, 1/08-12/10
<ul style="list-style-type: none"> • Served as guest lecturer, 11/11/09, 11/13/09, 11/10/10 • Led 1210 and 1220 general chemistry recitations/discussions. • Formatted questions for use with i-clicker response system. • Prepared, administered and graded weekly quizzes. • Prepared short lectures. • Taught general chemistry lab sections taken by high school students for college credit. • Utilized Blackboard/Vista online system. 	
Biochemistry Lab 3710/5710	1/11-
5/11	
<ul style="list-style-type: none"> • Prepared short, introductory lectures covering the techniques and theory of experiments. • Participated in the development of new enzyme kinetics lab experiment. 	
Department Chemistry Tutor – UW-Oshkosh – Oshkosh, WI	9/02-
12/04	
<ul style="list-style-type: none"> • Tutored General Chemistry, Organic Chemistry, Biochemistry and Quantitative Analysis. 	

HONORS

- Marjorie H. Gardner Teaching Award, Utah State University, 2006, 2010
- Graduate Student Senate Travel Award, 2009
- Lawrence H. Piette Endowed Graduate Student Scholarship, Utah State University, 2006
- Outstanding Senior Chemistry Student, UW-Oshkosh, 2004
- Chancellor's Academic Scholarship, UW-Oshkosh, 2000

RESEARCH PRESENTED

- Beighley, MA., Ensign, SA. Role of Histidine Residues in the Catalytic Mechanism of 2-Ketopropyl-CoM Oxidoreductase/Carboxylase from *Xanthobacter autotrophicus* Py2. Poster presentation at American Chemical Society National Meeting, 2009.
- Beighley, MA., Ensign, SA. Role of Histidine Residues in the Catalytic Mechanism of 2-Ketopropyl-CoM Oxidoreductase/Carboxylase from *Xanthobacter autotrophicus* Py2. Slide talk presented at Graduate Student Symposium, 2008.

PUBLICATIONS

- Kofoed MA, Wampler DA, Pandey AS, Peters JW, Ensign SA. Roles of the redox active disulfide, and histidine residues forming a catalytic dyad, in reactions catalyzed by 2-Ketopropyl-Coenzyme M Oxidoreductase/Carboxylase. 2011. *J. Bacteriol.* In Press.
- Boyd JM, Clark DD, Kofoed MA, Ensign SA. Mechanism of inhibition of aliphatic epoxide carboxylation by the Coenzyme M analog 2-bromoethanesulfonate. 2010. *J Biol Chem*, 285:25232-25242.